Chemiluminescence Enhanced by Quantum Dots from Peroxide Reactions and Its Application in Analytical Chemistry

December 2013

Zhou Yun

Akita University

Abstract

Chemiluminescence (CL) is a process of transforming chemical energy into light emission. It has been an attractive topic of intensive research over 100 years. Now it has developed to an important and powerful tool in biological and medical investigations. CL analysis is a powerful analytical technique. It has a cheap and simple optical detection system with low background noise, low detection limit, and wide working range. It has been proven effective in rapid and sensitive measurements at ultra-trace levels.

Quantum dots (QDs, or colloidal semiconductor nanocrystals (NCs)), have become the focus of research attention due to the unique size-dependent optical and electronic properties，and have been widely used in recent years. Compared to fluorescent semiconductor nanocrystals, photoluminescent carbon nanodots (C-dots) are superior in chemical stability, biocompatibility, and low toxicity.

Reactive oxygen species (ROS) are chemically reactive molecules containing oxygen. Examples include oxygen ions and peroxides. Recently, most research interests on ROS are focused on its effects on life science，medicine and environment.

In the present work, the CL of ROS originated from peroxide reactions with and without QDs and C-dots sensitizers and its analytical application were investigated. The CL mechanism of ROS was also studied. The contents were summarized as follows:

Chapter 1 The concept, principles and the development of investigation and application of CL, ROS, QDs sensitizers were introduced.

Chapter 2 Enhanced CL of peroxomonosulfate–cobalt (II) system in the presence of dicarboxylic acids. In this work, the effects of molecular mass aliphatic dicarboxylic acids on the HSO_5^--Co^{2+} CL system were investigated. It was found that the aliphatic dicarboxylic acids could enhance the CL of the HSO_5^--Co^{2+} system. Moreover, the CL intensities improved regularly with the increasing of the carbon chain length of the dicarboxylic acids. The enhancement of the CL should be attributed to the formation of peroxo-diacid, which finally decomposed to the original dicarboxylic acid and singlet oxygen. The mechanism of the HSO_5^--Co^{2+}-dicarboxylic acid CL system was then proposed.

Chapter 3 CL from NaClO-H_2O_2 and enhanced by l-cysteine capped Mn-doped ZnS quantum-dots. In this work, water-soluble L-cysteine capped Mn-Doped ZnS@Si quantum-dots (Zn-dots), a kind of sensitizer, were synthesized. It was found that this sensitizer could enhance CL signals emitted from interaction of NaClO with H_2O_2 in basic medium. Experimental results demonstrated that the CL enhancement of NaClO-H_2O_2 system originated from energy transfer processes occurred between an excited dimer singlet oxygen ($(^1O_2)_2^*$) and Zn-dots.

Chapter 4 Carbon nanodots sensitized CL on peroxomonosulfate-sulfite-hydrochloric acid system and its analytical application. In this work, new water-soluble fluorescent carbon nanodots (C-dots) were prepared in a facile microwave pyrolysis approach in minutes by combining glycine and polyethylene glycol 200 (PEG 200). It was discovered

that the prepared C-dots could dramatically enhance the CL intensity of potassium peroxymonosulfate- sodium sulfite-hydrochloric acid (PSHA) reactions. Experimental results indicated that the C-dots sensitized enhancements originated from their energy transfer and electron-transfer annihilation effects on the CL system. The C-dots sensitized CL system was successfully applied to the determination of aliphatic primary amines in real water samples with satisfactory results.

KEY WORDS: Reactive oxygen species, chemiluminescence, quantum dots, carbon nanodots, mechanism

Table of Contents

Chapter 1 Introduction

1 The introduction of ROS, CL, QDs and C-dots sensitizers

Reactive oxygen species (ROS) are chemically reactive molecules containing oxygen. Examples include oxygen ions and peroxides. ROS are molecules like hydrogen peroxide (H_2O_2), ions like the hypochlorite ion (ClO^-), radicals like the hydroxyl radical ($^{\bullet}OH$) and superoxide anion ($O_2^{\bullet-}$) which is both ion and radical. Hydroxyl radical is the most reactive of them all. Recently, most research interests on ROS are focused on its effects on life science，medicine and environment. ROS are formed by several different mechanisms:

1) The interaction of ionizing radiation with biological molecules.

2) As an unavoidable byproduct of cellular respiration. Some electrons passing "down" the electron transport chain leak away from the main path (especially as they pass through ubiquinone) and go directly to reduce oxygen molecules to the superoxide anion.

3) Synthesized by dedicated enzymes in phagocytic cells like neutrophils and macrophages.

In recent years, quantum dots (QDs, or colloidal semiconductor nanocrystals (NCs)), have stimulated great interest in many studies. With size-dependent novel electronic and optical properties, QDs developed the new fields within materials by offering with many attractive physical and chemical advantages [1-3]. Basically these advantages originated from the surface and quantum confinement effects of QDs, such as well chemical and photo stability, high adsorption characteristics, high emission quantum yields and etc. [4,5]

Compared to QDs, photoluminescent carbon nanodots (C-dots) also have been paid great attention in many fields [6,7]. They are discrete and almost spherical nanoparticles with sizes below 10 nm. They can be bought inexpensively and easily in bulk by many methods (for example, electrochemical oxidation of graphite or multiwalled carbon nanotubes, one-step pathway of microwave pyrolysis approach, etc.) [8,9]. They have many luminescent properties such as strong optical absorption in the UV region, photoluminescence produced with photoexcitation, and electrochemiluminescence (ECL) generated by electron injection [10]. They have many other amazing characteristics: size and wavelength-dependent luminescence emission, resistance to photobleaching, and ease of bioconjugation without toxicity and environmental hazard. Besides these outstanding advantages, the most commendable is that they are covered with hydrophilic hydroxyl of PEG 200 covered outside. Therefore they have good solublility in water, which greatly deepens their applications as many reactions occurring in aqueous phase systems [11].

Chemiluminescence (CL) is the emission of light, as the result of a chemical reaction (Figure 1). Given reactants A and B, with the excited C, light is given off as the excited C returns to ground state. Or the excited C passes its energy to F. F is a free matter, when the excited F returns to ground state, the CL light is given off (Figure 2).

Figure 1 A chemiluminescent reaction carried out in an Erlenmeyer flask producing a large amount of light (From Wikipedia, the free encyclopedia)

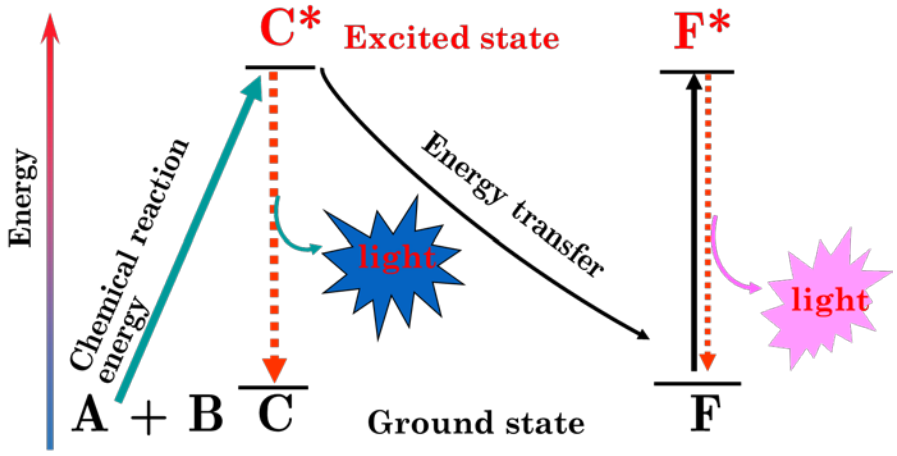

Figure 2 Schematic diagram of CL reaction processes

A CL-based analysis method was established before the latter half of the 20th century, although the first CL phenomenon was reported more than 100 years ago (12). With the appearance and development of the photomultiplier tube detector, the CL analysis method has been applied in many different fields, and now become a well-known powerful and important analytic technique (13). This technique has more prominent advantages such as high sensitivity and simple instrumentation than that of other common spectroscopic detection techniques (such as spectrophotometry and fluorescence analysis techniques) (14). For

example, the CL analysis technique requires no excitation source (as fluorescence or phosphorescence does), but a single light detector such as a photomultiplier tube with no monochromator and often not even a filter. Furthermore, the detection limit of CL analysis technique is 10 to 100 times lower than other luminescence techniques.

2 Development of nanomaterials in CL

Nanomaterials (NPs) have attracted a great deal of attention due to their fascinating properties and potential applications in nanotechnology and biotechnology. They have quantum size effects, high surface energy and large surface area, which dramatically changes their density states and the spatial scale of their electronic motion. They have catalytic properties duo to their size distribution, shapes and stabilizing agents, which are promising for signal amplification [15,16].

Now, NPs are widely incorporated with traditional CL analytic techniques in order to improve the detection sensitivity and the stability [17]. Originally, these NPs participating in CL reactions act as catalyst, reductant, luminophor or energy acceptor.

Semiconductor NPs, often referred to as quantum dots (QDs), have stimulated great interest in many studies. They have generated great fundamental and technical interest for their possible luminescent application in recent years [18]. Semiconductor NPs comprise a semiconductor-metal core surrounded by a coating of wider band-gap semiconductor metals. Their unique optical properties include sideband excitation, narrow emission, phenomenal

photostability and high quantum yield. The size-dependent emission is probably the most attractive property of QDs. Photoluminescence and electrogenerated CL of colloidal semiconductor nanocrystals in aqueous solution have been extensively investigated [19].

Recently, photoluminescent carbon nanodots (C-dots) have received much attention. These environmentally-friendly C-dots are usually prepared by laser ablation of graphite, electrochemical oxidation of graphite, electrochemical soaking of carbon nanotubes, thermal oxidation of suitable molecular precursors, vapor deposition of soot, proton-beam irradiation of nanodiamonds, microwave synthesis, and bottom-up methods.[7] They are discrete nanoparticles of near spherical geometry with sizes below 10 nm, and they inherently fluoresce in the visible upon light excitation. Compared to fluorescent semiconductor nanocrystals, photoluminescent C-dots are superior in chemical stability, biocompatibility, and low toxicity. [7] Their abundant surface traps and functional groups endowed them with bright, stable luminescence and excellent water dispersion. It was found recently that C-dots could enhanced the intensity of an ultra-weak CL from reaction of hydrogen peroxide and bisulfite and could also be used for nitrite sensing in a peroxynitrous-acid-induced CL. Coupled with their low cost, low cytotoxicity, and ease of labeling, promising applications in CL detection, biological labeling and biosensors are envisioned.

3 Research significance and contents

Though CL has been explored for many years and has been proved important in analytical chemistry, the usages of classical reagents, such as luminol,

lucigenin, peroxalate, potassium permanganate, and Ce (Ⅳ) in CL analysis suffered from expensive of poisonous reagents, poor selectivity, or narrow linear range. Meanwhile, the development of CL was limited in other CL reaction systems because the intensities of many reactions were not strong enough for applications. Therefore, it's necessary to develop some new CL systems with relatively cheap and green reagents. It's of very significant correspondingly to enhance the intensities of these CL systems for better analytical performances. In this work, three CL systems and the effects of QDs on CL systems and their analytical applications were investigated for the first time:

1) Enhanced CL of peroxomonosulfate-cobalt (II) system in the presence of dicarboxylic acids.

2) CL from NaClO-H_2O_2 and enhanced by Zn-dots.

3) C-dots sensitized CL on PSHA system and its analytical application.

To the best of our knowledge, PSHA CL system and Zn-dots and C-dots synthesized from amino acids were reported for the first time. Also the sensitizing effects and CL mechanisms of these new QDs on NaClO-H_2O_2 and PSHA CL systems were investigated for the first time. The effects of ROS on CL system were characterized by a variety of spectrographs. These researches not only broadened the applications of some novel materials but also had important instructions in method and theory for the studies on the mechanisms of ROS and the analytical applications of QDs sensitized CL systems in practice.

Chapter 2 Enhanced chemiluminescence of peroxomonosulfate–cobalt (II) system in the presence of dicarboxylic acids

1 Introduction

Peroxymonosulphurous acid (H_2SO_5, PMS, Caro's acid), a powerful oxidizing agent than the corresponding peroxydiacid ($H_2S_2O_8$) can be considered as a substituted hydrogen peroxide in which one of the hydrogen is replaced by an oxyanion group of sulfur. With $pK_{a1} < 0$, $pK_{a2} = 9.88 \pm 0.1$ at 15°C and electrode potential E=1.82 V vs. HSO_4^-, PMS is highly reactive. In aqueous solution around neutrality, PMS decomposes rapidly and readily oxidizes many inorganic reagents and attacks most organic compounds [20, 21]. So PMS is often used as an inorganic strong acid and a more powerful oxidant in the Baeyer-Villiger reaction, which allows the conversion of ketones into esters. Potassium peroxomonosulphate ($KHSO_5$), the inorganic salt of PMS is an inexpensive, commercially available potassium carotate. $KHSO_5$ exists in the form of potassium peroxomonosulphate triple salt ($2KHSO_5 \bullet KHSO_4 \bullet K_2SO_4$), which is prepared by the reaction of 86% H_2O_2 with concentrated H_2SO_4, followed by neutralization with K_2CO_3 [22]. $KHSO_5$ is also used as an oxidant in a wide range of oxidations such as oxidizing alcohols, ketones, carboxylic acids, alkenes, phenols, amines and sulphides [23]. HSO_5^- is stable in an acidic or basic solution except in the solution of pH =pK_{a2} [24], in which HSO_5^- decomposes rather rapidly to yield singlet oxygen ($^1O_2$) - a key role in the singlet oxygen ($^1O_2$) CL chemistry.

CL is the emission of light from the chemical reaction. A CL-based analysis

method was established before the latter half of the 20th century, although the first CL phenomenon was reported more than 100 years ago [25]. With the appearance and development of the photomultiplier tube detector [26-28], the CL analysis method has been applied in many different fields [29-31], and now become a well-known powerful and important analytic technique [32]. This technique has more prominent advantages such as high sensitivity and simple instrumentation than that of other common spectroscopic detection techniques (such as spectrophotometry and fluorescence analysis techniques) [33-35]. For example, the CL analysis technique requires no excitation source (as fluorescence or phosphorescence does), but a single light detector such as a photomultiplier tube with no monochromator and often not even a filter. Furthermore, the detection limit of CL analysis technique is 10 to 100 times lower than other luminescence techniques.

Generally, most CL methods involve only a few chemical components to actually generate light emission. Inorganic oxidants, such as peroxomonosulphate (HSO_5^-), persulphate ($S_2O_8^{2-}$), peroxymonocarbonate (HCO_4^-), and peroxynitrite ($ONOO^-$) were the chemical components used usually in CL system [36, 37]. For instance, Amir reported a flow injection method for the determination of L-cysteine, based on its enhancement on CL emission of luminol oxidized by sodium persulphate in alkaline solution [38]. In their work, persulphate, as an inorganic oxidant, was used. Compared with persulphate, PMS is more popular in CL analysis. As reported, PMS was susceptible to be catalyzed by trace amount of impurities in aqueous buffer

solutions [22]. In the presence of trace amounts of transition metal ions, such as Co (II) and Fe (II), a weak CL emission was observed while HSO_5^- reacted with the transition metal ions [25]. Among various transition metal ions, Co (II) was proven the best one to activate PMS to form radicals, including $SO_5^{\cdot-}$, $SO_4^{\cdot-}$ and ·OH. These radicals had already been identified by optical pulse radiolysis acting as key roles in some CL reactions [39]. As a CL analysis technique, the transition metal catalyzed CL analysis had already been employed in some application fields [25]. For example, Qiyong developed an inhibitive flow–injection CL method for the determination of rutin. In that method, tetrasulfonated cobalt phthalocyanine, a chelate with Co (II) as center, was used as mimetic enzyme to catalyze luminol-hydrogen peroxide CL reaction [40]. Unlike inorganic $CoSO_4$, tetrasulfonated cobalt phthalocyanine was previously synthesized by a sophisticated method before use.

Singlet oxygen ($^1O_2$), an excited state of molecular oxygen, is one of the most active intermediates involved in chemical and biochemical reactions. It is particular concerned in various CL reactions by chemists. $^1O_2$ CL, for instance, has been extensively applied for analytical purposes in chemistry and biochemistry. Since 1960s, especially during the last few decades, the $^1O_2$ CL has been extensively studied [41]. The monomol and dimol CL of $^1O_2$ have made a sustaining impact on oxidation chemistry and provided important information on the mechanism of light generation in peroxide reactions [42-44]. Now, the $^1O_2$ CL has become a convenient and powerful tool in the kinetic studies and accounting for the light emission in biological and chemical

systems.

As reported in our early research, hydrocarbons, like low molecular mass aliphatic monocarboxylic acids (formic, acetic, propionic, butyric and valeric acids), improved the CL emission of HSO_5^--Co^{2+} system dramatically [22]. In present study, to further investigate the influence of aliphatic acids on HSO_5^--Co^{2+} CL system, the CL of the interaction of low molecular mass aliphatic dicarboxylic acids with HSO_5^--Co^{2+} system were first investigated. In addition, the effects of some organic solvents on HSO_5^--Co^{2+}-dicarboxylic acid CL system were also studied. These aliphatic dicarboxylic acids included oxalic acid, malonic acid, succinic acid, glutaric acid, hexane diacid, and pimelic acid. The possible CL mechanism was then proposed based on study of the dynamic kinetic curve of the CL reaction, the quenching of NaN_3, the effects of some organic solvents, the CL spectrum and ESR spectrum.

2 Experimental

2.1 Reagents and materials

All reagents were of analytical grade and used as received. Water was purified using a Compact Ultrapure water system (18.3 MΩ/cm; Millipore, Barnstead, CA, USA). Solutions of $KHSO_5$ available in the form of a triple salt (K_2SO_4•$KHSO_4$•$2KHSO_5$) as Oxone (Alfa, Ward Hill, USA) and cobalt (II) sulphate ($CoSO_4$) (Beijing Chemical Reagent Company, Beijing, China) were prepared daily. Five low molecular mass aliphatic dicarboxylic acids, malonic acid, succinic acid, glutaric acid, hexane diacid and pimelic acid were from

Beijing Chemical Company (Beijing, China) and Alfa (Ward Hill, USA). The selected organic solvents, soluble in water, were also from Beijing Chemical Company (Beijing, China).

2.2 Apparatus

The schematic diagram of the flow injection system used in this work was shown in Figure 1. The two peristaltic pumps (Xi'an Remex Analytic Instrument CO. LTD. Xi'an, China) were used. One of the pumps was used to deliver the flow streams of $KHSO_5$ and $CoSO_4$, and the other was used to deliver the sample solution or the water. PTFE tubing (0.8 mm i.d.) was used as connection material in the flow system. The flow cell, placed close to the photomultiplier tube (PMT) window, was a flat spiral-coiled colorless glass tube (1.0 mm i.d.; total diameter of the flow cell, 3 cm, without gaps between loops). The potassium peroxomonosulphate solution and cobalt sulphate solution were mixed first in a three-way valve, and then merged with the stream of sample solution in a six-way valve. The merged solution, driven by the pump, flowed immediately into the flow cell, from where the CL light of chemical reaction was emitted. The CL signal produced from the flow cell was collected with a CR-105 PMT (Hamamatsu, Tokyo, Japan, operated at −800 or 850 V) of the IFFM-E CL Analyzer (Xi'an Remex Analytic Instrument CO. LTD. Xi'an, China). Date acquisition and treatment were performed with IFFM-E analysis client system. The CL mechanism was investigated in detail by electron spin resonance (ESR) spin trapping technique, the quenching of NaN_3, the fluorescence spectrum and the CL method.

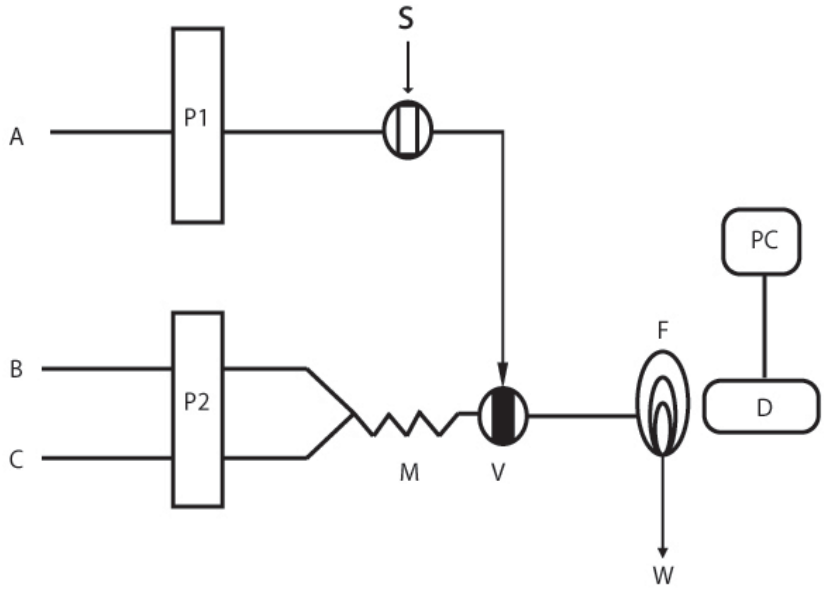

Figure 1. Schematic diagram of the flow injection system: A, water; B, $KHSO_5$; C, $CoSO_4$; S, sample; P1and P2, peristaltic pump; M, mixing tube (1.0mm i.d.×20cm); V, six-way valve; F, CL flow cell; W, waste; D, PMT detector; PC, compatible computer.

2.3 Optical measurements

ESR spectroscopy was used to detect the existence of singlet oxygen in the CL reaction. The ESR measurements were obtained with ESP-300E spectrometer (Bruker, USA) working at room temperature. The microwave frequency and the modulation amplitude were 9.75GHz and 1.04G respectively. The radical trapper, TEMP (assay≥99%, 3μL) was dissolved in 100L mixed sample solution. The delicate quartz pipe filled by capillarity with the mixed solution was placed then in the cavity of the ESR spectrometer.

2.4 Procedures for CL detection

As shown in Figure 1, sample solution (labeled as S, with 1.2mL/min sample rate) was delivered by the pump P1 and then mixed with the solution of 4.0 ×

10^{-3}mol/L $KHSO_5$ and 1.0 × 10^{-2}mol/L $CoSO_4$ by means of a six-way valve and finally flowed into in the flow CL cell. As reported, the CL signal would reach its maximum at about 3 min after the mixing, which means a 20 cm mixing tube was enough to optimize the mixing degree (3). The CL intensity vs. time curve was recorded consecutively by workstation. And the CL intensity of $KHSO_5$ and $CoSO_4$ mixture solution without sample injection was recorded as blank signal. The CL intensity of sample was quantified by the increased CL intensity $\Delta I = I_s - I_b$, where I_s was the CL intensity of sample solution, and I_b was the blank signal. With optimized reaction conditions, the increased CL relative intensity (ΔI) was corresponded to the normal maximum light intensity.

3 Results and discussion

3.1 Design of flow-injection CL system

A rational mixing means (i.e. mixing order and mixing time interval) of reagents and the speeds of the CL reaction should be taken, which were of great importance for the design of the flow-injection CL system and accordingly had great effect on the CL intensity. Generally, different CL intensities depend on different mixing ways and the speeds of the CL reaction. And sometimes, no or very weak CL intensity will be observed on the irrational mixing means or the speeds of the CL reaction. Being very transient for the light emission from CL reaction, the speed of the CL reaction was a dominant factor in deciding the sensitivity in flow-injection CL system. In order to measure the intensity of CL at maximum sensitivity, the intensity–time profile of this CL system was

examined by a batch method. The results shown that the rate of the CL reaction of HSO_5^- and Co^{2+} solution was very fast: the CL intensity reached a maximum at 2s after initiating the reaction, and decayed to baseline within 5s. More experiments indicated that the mixing order of the reagents should be designed as follows: first the mixing of $KHSO_5$ with $CoSO_4$ solution and then mixing with sample in the flow CL cell.

3.2 Dynamic profile of CL

The chemiluminescent dynamic profile of HSO_5^--Co^{2+}- dicarboxylic acids CL system was recorded (Figure 2). The CL signal of HSO_5^--Co^{2+} without other reagents was recorded as blank CL intensity. As shown in the CL kinetic curve, a weak luminescence was yielded when $CoSO_4$ was injected into the $KHSO_5$ solution. A strong CL was then observed when low molecular mass aliphatic dicarboxylic acid was added into the HSO_5^-/Co^{2+} solution system. From Figure 2, it was found that all the CL reached its maximum intensity at about 2s, which meant that the reaction of HSO_5^- with Co^{2+} was a fast CL process. On the other hand, compared with the blank signals, the duration of the CL signals was obviously enhanced from 50s to nearly 300s, and the CL intensity was correspondingly enhanced dramatically from 118 counts to nearly 1200 counts.

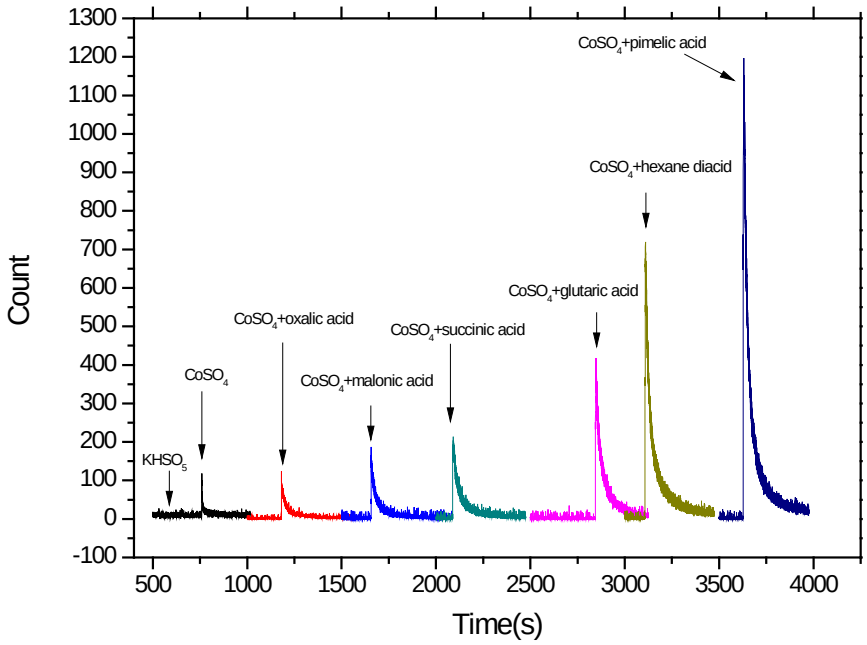

Figure 2. Dynamic profiles of CL for $KHSO_5$, $CoSO_4$, and aliphatic dicarboxylic acids. The concentrations of $KHSO_5$, $CoSO_4$ and dicarboxylic acids were 1.0×10^{-2}, 1.0×10^{-2} and 1.0×10^{-3}mol/L, respectively. The injected volume of $KHSO_5$, $CoSO_4$ and dicarboxylic acids were all 50μL.

3.3 Optimization of the experimental conditions

The experimental conditions of HSO_5^--Co^{2+} CL system were optimized as results shown in Figure 3. The CL intensity with different mixing tube length was measured. The results demonstrated that the CL intensity decreased dramatically with the increasing of mixing tube length (Figure 3A). It was probably due to the catalytic decomposition of peroxymonosulphate, which implied the necessary to shorten mixing tube length as far as possible. Finally, the mixing tube was then designed as peroxymonosulphate mixed with Co (II) at the entrance of the flow CL cell. The effect of flow rate was tested in the

range of 0.1-1.5mL/min for each stream and the selected succinic acid was at 1.0×10^{-6}mol/L; the result was shown in Figure 3B. The CL intensity increased with the increasing flow rates of $KHSO_5$ and $CoSO_4$ from 0.1 to 0.6 mL/min. Over 0.6 mL/min, the CL intensity decreased gradually. The flow rate of carrier stream behaved similar trend with 0.6 ml/min which was the best one among the rates investigated. Therefore, the optimized flow rate condition for the HSO_5^-/Co^{2+} CL system was 0.6ml/min for all streams. The effects of concentrations of $KHSO_5$ and $CoSO_4$ were investigated in the range of 5.0×10^{-4}-1.0×10^{-2}mol/L (results were shown in Figure 3C and Figure 3D). The CL intensity enhanced steadily when the concentrations of $KHSO_5$ and $CoSO_4$ were increased from 5.0×10^{-4}mol/L to 6.0×10^{-3}mol/L; then the CL intensity decreased gradually when the concentration was over 6.0×10^{-3}mol/L. The concentration of 6.0×10^{-3}mol/L was finally chosen as of $KHSO_5$ and $CoSO_4$.

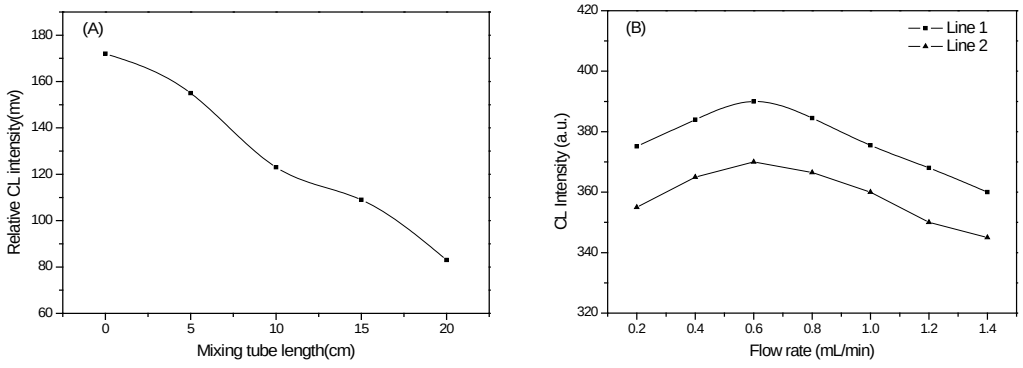

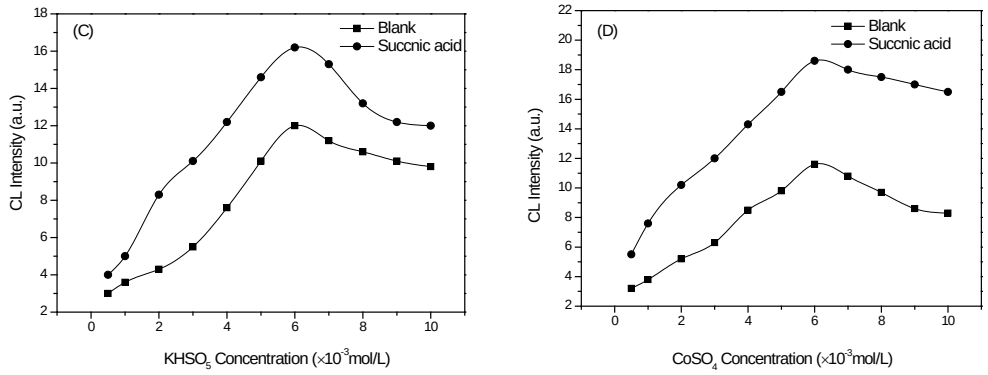

Figure 3. Optimization of the experimental conditions. (A) Effect of mixing tube length: 1.0×10^{-2}mol/L $KHSO_5$, 1.0×10^{-2}mol/L $CoSO_4$. (B) Effect of flow rate: 5.0×10^{-3}mol/L$KHSO_5$ and $CoSO_4$, 1.0×10^{-4} mol/L succinic acid; Line 1, effect of flow rate of $KHSO_5$ and $CoSO_4$, 1.0mL/min carrier stream; Line 2, effect of the flow rate of carrier stream, 1.0mL/min $KHSO_5$ and $CoSO_4$. (C) Effect of $KHSO_5$ concentration: 1.0×10^{-4} mol/L succinic acid, 1.0×10^{-2} mol/L $CoSO_4$; flow rate of $KHSO_5$ and $CoSO_4$, 0.6mL/min. (D) Effect of $CoSO_4$ concentration: 1.0×10^{-4}mol/L succinic acid, 4.0×10^{-2} mol/L $KHSO_5$; flow rate of $KHSO_5$ and $CoSO_4$, 0.6mL/min.

3.4 Flow injection CL under the optimum conditions

Five aliphatic dicarboxylic acids aqueous solutions, oxalic acid, malonic acid, succinic acid, glutaric acid, hexane diacid, and pimelic acid solutions were studied by FIA technique. Figure 4 showed the FIA CL signals for the CL system when added with aliphatic dicarboxylic acids under the optimized conditions. The results indicated that with the increase of carbon chain length, the CL intensities of the aliphatic dicarboxylic acids were enhanced gradually in the HSO_5^--Co^{2+} system.

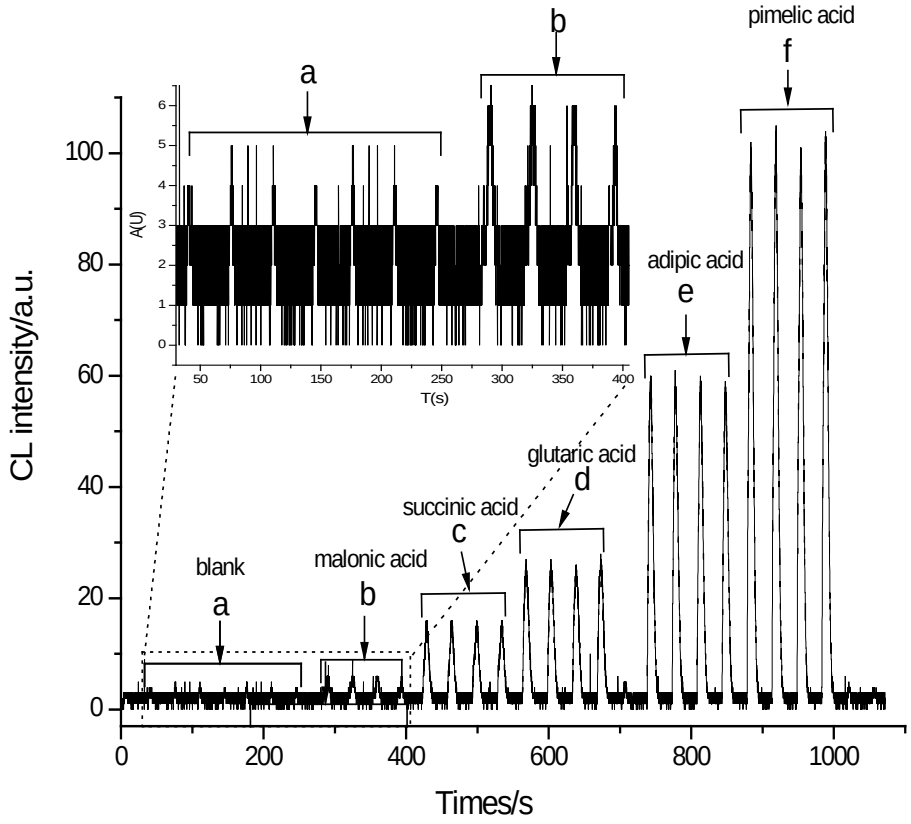

Figure 4. CL signals for (a) oxalic acid, (b) malonic acid, (c) succinic acid, (d) glutaric acid, (e) hexane diacid, and (f) pimelic acid. The concentrations of $KHSO_5$, $CoSO_4$, and aliphatic dicarboxylic acids were 6×10^{-3}, 6.0×10^{-3} and 1.0×10^{-4} mol/L, respectively. The flow rates of $KHSO_5$ solution, $CoSO_4$ solution and carrier (water) were all 0.6 mL/min.

3.5 Effects of organic solvents

As introduced in our previous work [25], some organic solvents, such as surfactant micelles or water-miscible organic solvents all suppressed the CL signals of HSO_5^--Co^{2+} system. In present study, some organic solvents were investigated (Figure 5). Among the investigated solvents, methanol had the strongest suppress effects on the HSO_5^--Co^{2+}- dicarboxylic acids CL system. Figure 5A showed the suppress profile of methanol on the CL system with

hexane diacid added. Figure 5B showed all the suppress effects of methanol on the CL system with seven dicarboxylic acids added (effects data of other solvents on the CL system not shown). Figure 5C showed that, when added with low polar solvents (n-hexane and chloroform), there were no evident effects on the CL signals of HSO_5^--Co^{2+} system; but when added with the solvents with dielectric constant over 20, the CL intensity decreased dramatically especially.

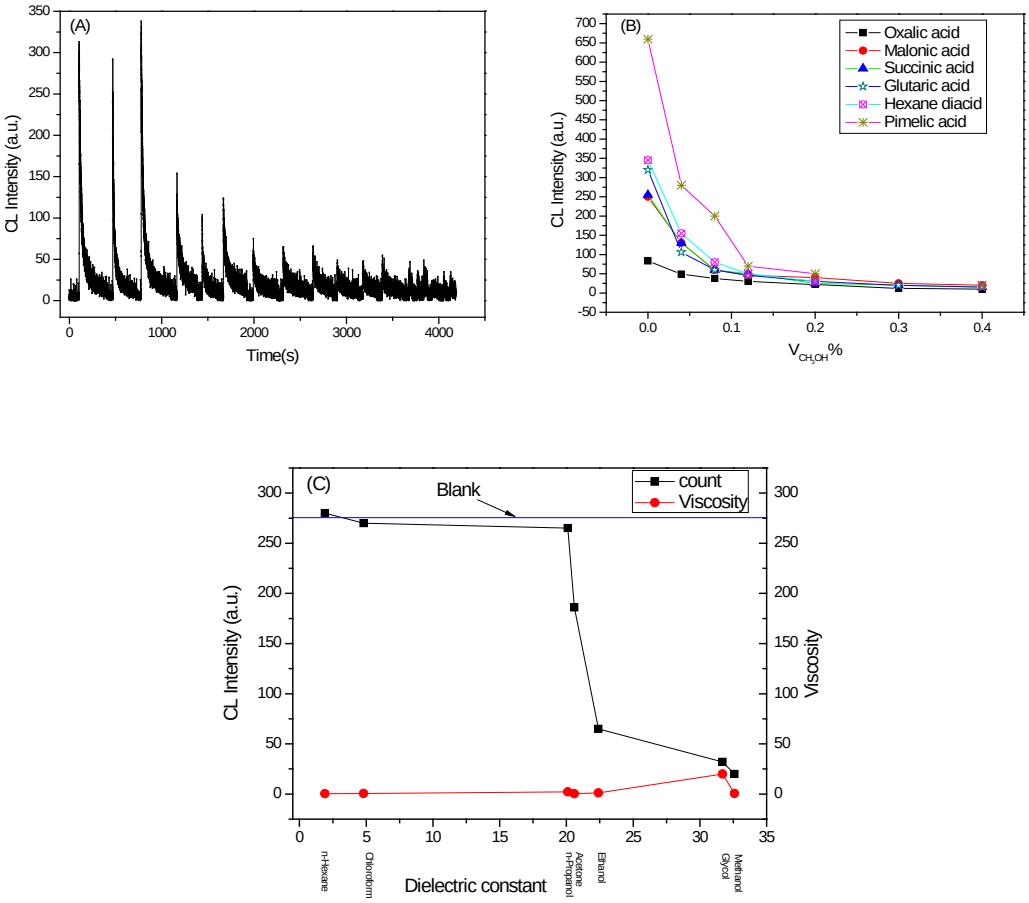

Figure 5. Effect of organic solvent. (A) CL profiles in batch studies: 0%, 0.04%, 0.08%, 0.12%, 0.2% and 0.4% Methanol (V/V), 1×10^{-2}mol/L $KHSO_5$, 1×10^{-2}mol/L $CoSO_4$ and 1×10^{-3}mol/L hexane diacid. (B) Effect of methanol concentration: 1×10^{-2}mol/L $KHSO_5$, 1×10^{-2}mol/L $CoSO_4$, 1×10^{-3}mol/L dicarboxylic acid. (C) Line 1: Effects of organic solvents with different

polarities, 1×10^{-2}mol/L $KHSO_5$, 1×10^{-2}mol/L $CoSO_4$, 1×10^{-3}mol/L dicarboxylic acid; Line 2: viscosities of variant organic solvents.

3.6 Quenching effect on the CL system

There were many reports on the mechanism of HSO_5^- reacting with Co^{2+}. Generally opinions confirmed that singlet oxygen ($^1O_2$), an excited state of molecular oxygen, played a very important role in the CL reactions. Singlet oxygen was generated during the decomposition of HSO_5^- in the presence of trace amounts of Co^{2+}. To confirm the role of $^1O_2$, the known quencher of $^1O_2$, NaN_3, was used [25]. Figure 6 showed the effective quench effect of NaN_3 on the CL system. The existence of $^1O_2$ was proved adequately during the decomposition of HSO_5^-. To further confirm the generation of $^1O_2$ in this CL reaction, electron spin resonance (ESR) spin trapping technique and the CL spectra were employed.

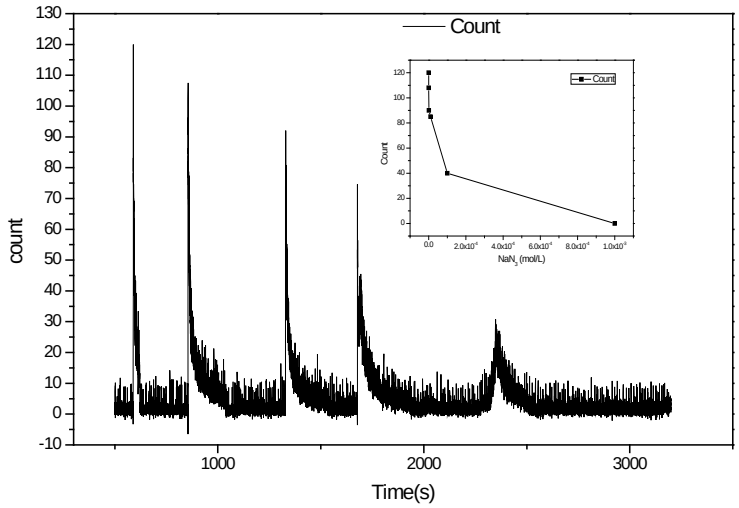

Figure 6. Effect of NaN_3 on the CL signals. Batch method: 50μL of 1.0×10^{-2} mol/L $KHSO_5$ solution was injected into 50μL of 1.0 10^{-2} mol/L $CoSO_4$ solution containing NaN_3.

3.7 ESR spin –trapping with 2, 2, 6, 6-tetramethyl 1-4-piperidine

Figure 7 showed the specific signals of TEMPO, which was produced by the reaction of TEMP with singlet oxygen. Spectrum 2 indicated the generation of singlet oxygen in the $KHSO_5$-$CoSO_4$ CL system, spectrum 3 and 4 showed the suppress effect of 0.1% (V/V) and 0.02% (V/V) methanol, while the spectrum 5 showed the enhancement effect of 1×10^{-3} mol/L hexane diacid on the CL system. The results indicated firmly that the singlet oxygen was generated during the CL reactions.

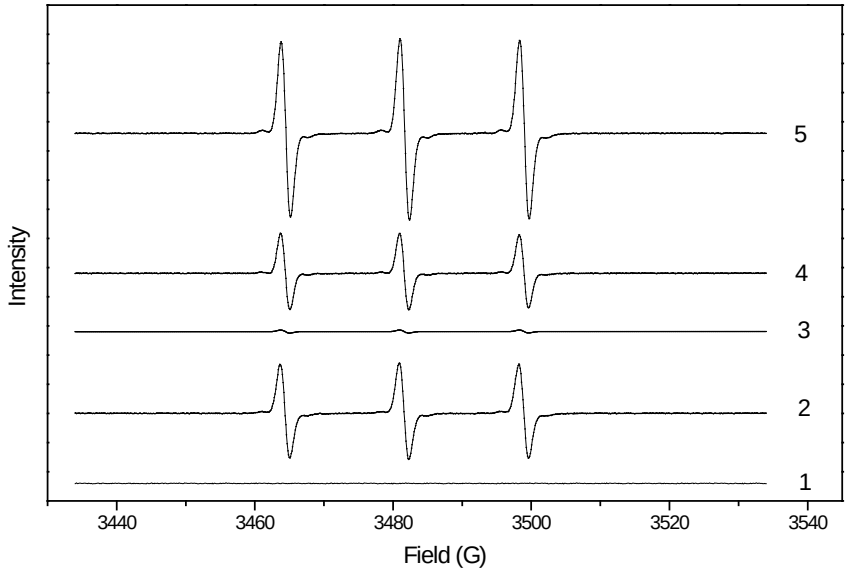

Figure 7. ESR spectra of singlet oxygen by reaction of TEMP with the CL system. Spectrum 1, blank (H_2O); spectrum 2, $KHSO_5$-$CoSO_4$ CL system; spectrum 3, 0.1% (V/V) methanol added in $KHSO_5$-$CoSO_4$ CL system; spectrum 4, 0.02% (V/V) methanol added in $KHSO_5$-$CoSO_4$ CL system and spectrum 5, 1×10^{-3} mol/L hexane diacid added in $KHSO_5$-$CoSO_4$ CL system. Conditions: receiver gain=8.00e+04; Modulation amplitude=1.04G; Sweep width=100.00G; Microwave frequency=9.7500GHz.

3.8 Proposed CL mechanism

It has been proved that many transition metal ions could act well as catalyst in many chemical reactions [45].Among these transition metal ions, Co (II) was the best one as catalyst to peroxymonosulphate [1]. Also the catalytic performance of Co (II) to the decomposition of peroxymonosulphate had been reported [46-47].

In order to well understand the CL mechanism of HSO_5^--Co^{2+}-dicarboxylic acid system, the effects of various organic solvents were investigated. The results were shown in the Figure 5. It had been reported that aqueous-phase $^{\cdot}OH$-attack on one of the H-atoms linked to the carbon atom of methanol was dominant (with a yield of 93%, Reaction 1) [48]. One production of this radical reaction was organic radical, which was rapidly oxidized by O_2 to produce hydroxymethyl peroxy radical (Reaction 2). The behavior of the peroxy radical was less certain. A slow unimolecular decomposition leading to formaldehyde had been observed (Reaction 3) [49]. Then the O_2 was generated from continuous reactions (Reactions 4-5), which finally reacted with hydroxymethyl radical (Reaction 2). Due to the hydroxyl radical was the key factor in the CL emission (Reactions 12, 15), the consumption of hydroxyl radical by methanol would suppress the CL signals of HSO_5^--Co^{2+} system inevitably. Moreover, the suppressant would be more severe with the increasing of the addition of methanol.

$$CH_3OH + \cdot OH \longrightarrow \cdot CH_2OH + H_2O \quad (1)$$

$$\cdot CH_2OH + O_2 \longrightarrow \cdot OOCH_2OH \quad (2)$$

$$\cdot OOCH_2OH \longrightarrow HCHO + \cdot HO_2 \quad (3)$$

$$\cdot HO_2 + \cdot HO_2 \longrightarrow H_2O_2 + O_2 \quad (4)$$

$$2\,H_2O_2 \longrightarrow 2\,H_2O + O_2 \quad (5)$$

When dicarboxylic acid was added to the HSO_5^--Co^{2+} CL system, as shown in Figure 4, the CL signal was enhanced dramatically. Reports had indicated that the aliphatic acid could react with hydrogen peroxide in an equilibrium process with a peroxo-diacid produced (Reaction 6) [50].

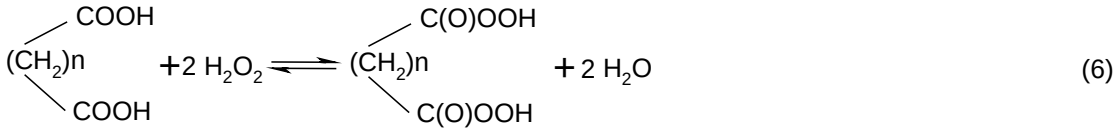

(6)

The anion HSO_5^- could also act as an oxidant to provide hydroxyl radical just like hydrogen peroxide (Reactions 7-8) behaved [23].

$$HSO_5^- \longrightarrow SO_4^{\cdot -} + \cdot OH \quad (7)$$

$$H_2O_2 \longrightarrow \cdot OH + \cdot OH \quad (8)$$

So HSO_5^- could oxide dicarboxylic acid to peroxo-diacid which was unstable and readily to undergo decomposition [51]. Though the peroxy-formic acid could probably degrade in two different means (Reactions 9-10), there were no evident characteristic peaks of carbon dioxide in the CL spectra proving the production of carbon dioxide [22].

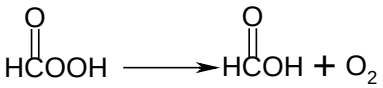

(9)

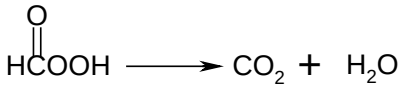

(10)

In short, the quench effect of NaN_3 on O_2 (Figure 6), the ESR spectra of TEMPO (Figure 6) and the characteristic peaks of oxygen in the CL spectra

(Figure 8) all proved the generation of oxygen in the CL reaction.

In equation 1, methanol, after added into the CL system, consumed hydroxyl radical which would quench the CL reaction. But the quench was not 100% as demonstrated in figure 5B for the existence of $SO_5^{\bullet-}$ radical. The $SO_5^{\bullet-}$ radical was produced during the interaction of HSO_5^- and Co (Ⅱ) (equations 13, 14, and 15). Meanwhile, in equations 12 and 15, hydroxyl radical could contribute partially to the production of $SO_5^{\bullet-}$ radical which promoted the formation of peroxo-diacid. During the formation of $SO_5^{\bullet-}$ radical, HSO_5^- played as a very important role as Co (Ⅱ) did in the CL reactions. Due to the oxidation potential of peroxomonosulfate (1.82V) was slightly higher than that of Co^{3+} ($E_{Co^{3+}/Co^{2+}}$=1.802V) [25], HSO_5^- oxidized Co^{2+} to produce $SO_4^{\bullet-}$ radical and Co^{3+} as shown in equation 11. Co (Ⅱ), as one of effective metal ion-catalysts [52], was reproduced again by the interaction of HSO_5^- and Co^{3+} (equation 13) [25]. $SO_5^{\bullet-}$ radical could oxidize dicarboxylic acids easily to form peroxo-diacid (Reaction 16). The peroxo-diacid decomposed in the only way as formic acid behaving (Reaction 9), i.e., decomposed to the original dicarboxylic acid and singlet oxygen at the same time (Reaction 17). Then, a singlet oxygen molecular pair, $(^1O_2)_2^*$, was formed with higher energy than that in its ground state triple oxygen [53-54]. In about 1×10^{-8} s, $(^1O_2)_2^*$ decayed quickly to O_2 with energy state decayed from excited state to the ground state. The CL emission from the decay formed the CL signal with emission bands in the VIS region: at around 545, 580, 634 and 703nm (Reaction 18) [45].

As shown in the CL dynamic profiles (Figure 2), the CL duration enhanced

with the increase of carbon chain length. The CL enhancement, to some degree, was highly correlated with the carbon numbers of the dicarboxylic acid. As reported, the CL intensity of the HSO_5^--Co^{2+}-dicarboxylic acid system was determined by the decomposition rate of the dicarboxylic acid. The decomposition rate of dicarboxylic acid, on the other hand, was hastened with the increase of the carbon chain length [55]. Therefore the CL intensity was enhanced regularly with the increase of carbon chain length (Figure 4). The CL mechanism of HSO_5^--Co^{2+}-dicarboxylic acid system, based on the discussion above, could be summarized as shown in Scheme 1:

Scheme 1: CL mechanism for HSO_5^--Co^{2+}-dicarboxylic acid system

$$HSO_5^- + Co^{2+} \longrightarrow SO_4^{\bullet -} + Co^{3+} + OH^- \quad (11)$$

$$HSO_5^- + Co^{2+} \longrightarrow SO_4^{2-} + Co^{3+} + OH^{\bullet} \quad (12)$$

$$HSO_5^- + Co^{3+} \longrightarrow HSO_5 + Co^{2+} \quad (13)$$

$$HSO_5^- + SO_4^{\bullet -} \longrightarrow SO_5^{\bullet -} + HSO_4^- \quad (14)$$

$$HSO_5^- + \cdot OH \longrightarrow SO_5^{\bullet -} + H_2O \quad (15)$$

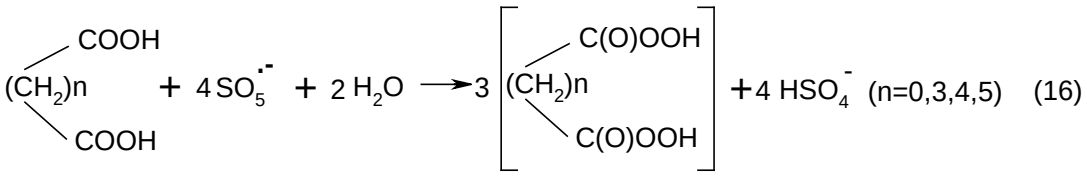

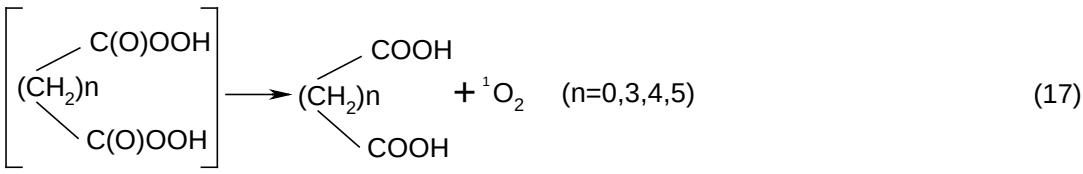

$$^1O_2 + {}^1O_2 \longrightarrow (^1O_2)_2^* \longrightarrow 2\,O_2 + h\nu \quad (18)$$

4 Conclusions

In conclusion, aliphatic dicarboxylic acids, such as oxalic acid, malonic acid, succinic acid, glutaric acid, hexane diacid and pimelic acid were found to enhance the $KHSO_5$-$CoSO_4$ CL signals. The CL enhancement of dicarboxylic acid might be attributed to the formation of peroxo-diacid, an unstable excited state, which finally decomposed to dicarboxylic acid and singlet oxygen. Moreover, the CL intensity was determined by the decomposition rate, which was improved with the increase of the carbon chain length. The CL signals were enhanced regularly with the increase of the carbon chain length. The CL emission was finally detected when the dimer $(^1O_2)_2^*$ being formed from singlet oxygen decayed to the triplet oxygen, a ground state species. Some organic compounds such as methanol were found to suppress the CL emission dramatically due to the scavenging of hydroxyl radical to $KHSO_5$-$CoSO_4$ system by methanol. This work was important for the CL mechanism investigation of $KHSO_5$-$CoSO_4$-dicarboxylic acid system.

Chapter 3 Chemiluminescence from NaClO–H_2O_2 and enhanced by l-cysteine capped Mn-doped ZnS quantum-dots

1 Introduction

Recently, quantum dots (QDs, or colloidal semiconductor nanocrystals (NCs)), have stimulated great interest in many studies. With size-dependent novel electronic and optical properties, QDs developed new fields in material science offering many attractive physical and chemical applications [57-61]. Basically these advantages originated from the surface and quantum confinement effects of QDs, such as good chemical and photo stability, high adsorption characteristics[62-66].

Being an intriguing research field, CL has been investigated for many years and is usually researched as an effective means gaining insight into chemical reactions and widening applications associated with it [67-70]. However, it's a challenging today to explore novel CL-reaction strategies providing new approaches to enhance the inherent sensitivity of CL techniques to widen and deepen its applications. Amongst a variety of new materials, nanomaterial is introduced into the CL system as the most promising to improve sensitivity and stability of CL. A recent challenging research field is the use of nanomaterial as a kind of catalyst, reductant, luminophor, or energy accepter in CL system [71-73]. Nanoparticles and QDs, with their excellent physical and chemical characteristics, have already been explored widely in CL reactions. As a reductant, CdTe NCs and CdS NCs were reported in CL reactions being directly

oxidized by some oxidants such as H_2O_2 and $KMnO_4$ [74, 75]. As catalysts involved in CL reactions, nanoparticles and QDs have also been reported. Gold nanoparticles of different sizes, for example, were found being used as a catalyst to promote CL-emission of KIO_4-Na_2CO_3/NaOH system, lucigenin-KI and luminol-H_2O_2 systems [76, 77]. In our previous work [78], gold nanoparticles were also used to catalyze the CL reactions of peroxymonocarbonate-eosin Y system and a dramatic enhancement of CL signals was obtained. As an energy acceptor, CdTe QDs performed a highly efficient CL resonance energy transfer from luminol (energy donor) to horseradish peroxidase (HRP)-QD conjugates and immuno-reaction of QD-BSA (bovine serum albumin) and anti-BSA-HRP in the luminol-H_2O_2 CL system [79]. CdTe QDs, a novel type of semiconductor, as another example, were first reported to conjugated with luminol for the investigation of CL resonance energy transfer, which is helpful for the insight into QDs and CL reactions [80]. Many more QDs have now been widely used as fluorescence biological probes [81], donors or acceptors of fluorescence resonance energy transfer [82], and probes in bio-imaging [83].

Generally, most weak luminescence originates from low quantum efficiencies and can be greatly enhanced by some QDs sensitizers. This CL enhancement was brought about by an energy transfer process from a donor of an excited species to an acceptor of sensitizer forming a new excited species. Finally, the excited sensitizer emits the characteristic radiation when it returns to its ground state. The energy transfer process is of great significance to explore the novel

CL behavior of semiconductor QDs for developing novel CL sensors.

In the present study, the sensitizing effects of Zn-dots on NaClO-H_2O_2 weak CL system were first investigated. Combined with flow-injection technique, it was found that, the CL signals of the NaClO-H_2O_2 system were enhanced dramatically by the sensitizer Zn-dots. The possible mechanism on NaClO-H_2O_2 CL system induced by the sensitizer of Zn-dots was then proposed.

2 Experimental section

2.1 Reagents and materials

All reagents were of analytical grade and used as received. Water was purified using a Compact Ultrapure water system (18.3 MΩ.cm; Millipore, Barnstead, CA, USA). Working solutions of H_2O_2 were prepared fresh daily by dilution of a 30% (v/v) H_2O_2 (Shanghai Taopu Chemical Company, China). A 1.0×10^{-3} mol/L stock solutions of NaClO (Beijing Chemical Reagent Company, Beijing, China) were prepared daily by diluting 6.767 ml of reagent solution (Containing 7-10% active chlorine) in 100 ml of redistilled water. Stock slutions of L-cysteine (3.0×10^{-1} mol/L), $ZnSO_4\cdot7H_2O$ (5.0×10^{-1} mol/L), $MnCl_2\cdot4H_2O$ (2.5×10^{-2} mol/L), and $Na_2S\cdot9H_2O$ (5.0×10^{-1} mol/L) were prepared by dissovling corresponding reagents (obtained from Sigma-Aldrich Co. (USA), Tianjin Kaitong Chemicals Co. (Tianjin, China), the Second Chemicals Co. of Shenyang (Shenyang, China), and Tianjin Sitong Chemicals Co. (Tianjin, China), respectively) in double-distilled water. Tetraethoxysilane (TEOS,

assay≥98%), 5, 5-dimethyl-1-pyrroline-N-oxide (DMPO, assay≥99%), and 6, 6-tetramethyl 1-4-piperidine (TEMP, assay≥99%) were all from Sigma-Aldrich Co. (USA).

2.2 Apparatus

Batch CL measurements were carried out with BPCL ultra weak CL analyzer (Institute of Biophysics, Chinese Academy of Science, Beijing, China) using a 3 mL quartz glass cuvette (Fig. 1A). The solution interval and the PMT work voltage were 0.01 s and -1.2 kV respectively. The flow injection CL system consisted of a flow CL analyzer (Lumiflow LF-800, Microtech NITI-ON, Funabashi, Japan) and two peristaltic pumps as shown in Fig. 1b. UV-vis absorbance spectra were performed in 1 cm quartz optical cells with a UV-2100s Spectrophotometer (Shimadzu, Japan). ESR measurements were obtained with a Bruker ESP-300E spectrometer working at room temperature. The microwave frequency and the modulation amplitude were 9.75 GHz and 1.04 G respectively. The radical trapper, solutions of 3 μL 5, 5-dimethyl-1-pyrroline-N-oxide and 3 μL 6, 6-tetramethyl 1-4-piperidine were dissolved into solution of 100 μL sample. The delicate quartz pipe filled by capillarity with the mixed solution was then placed in the cavity of the ESR spectrometer.

The phase purity of the product was verified by powder X-ray diffraction (XRD) on a Bruker D8 Advance X-ray diffractometer using Cu Kα radiation (λ = 1.5418 Å). The X-ray source was operated at a power of 40 kV×100 mA. Scanning speed was 0.1 deg/s and scanning step was 0.02º. The sizes and

morphologies of the nanocrystal were measured using a transmission electron microscope (TEM, JEM-1200EX, JEOL LTD, Japan) at 120 kV. Samples to be scanned with TEM were prepared by dispersing a drop of the dried Zn-dots in ethanol on the copper mesh for TEM observation.

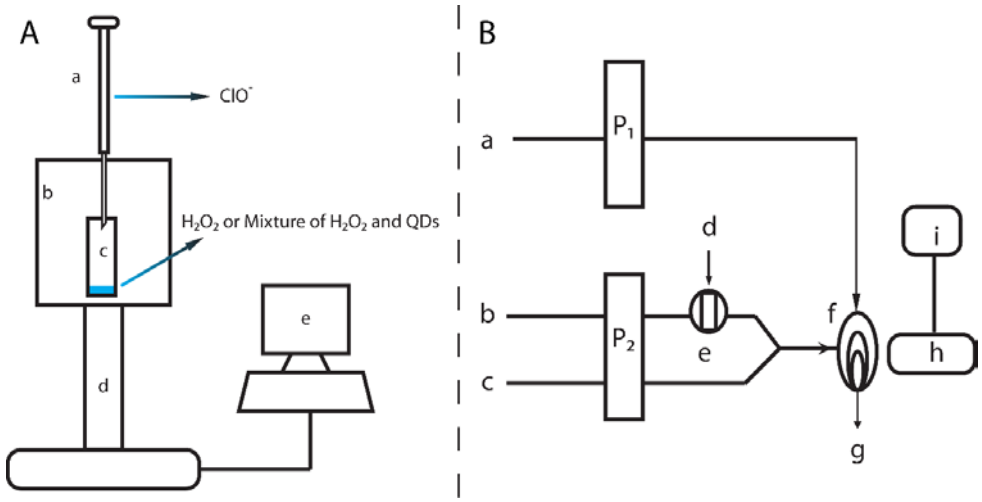

Fig. 1. Schematic diagram of CL analysis system. (A) Batch CL system: a, syringe loaded with solution of NaClO; b, darkroom; c, quartz glass cuvette loaded preliminary with mixture of aqueous colloid solutions of QDs and H_2O_2; d, PMT detector; e, computer; (B) Flow injection analysis system: a, solution of NaClO; b, carrier water; c, solution of H_2O_2; d, aqueous colloid solutions of QDs; e, six-way valve; f, CL flow cell; g, waste; h, PMT detector; i, computer; P_1 and P_2, peristaltic pump.

2.3 Procedures for CL detection

The schematic diagrams of batch and flow injection systems are shown in Fig. 1A and 1B respectively. In Fig. 1A, a mixture of 100 µL H_2O_2 and 100 µL water or QDs in aqueous colloid solutions was firstly added by an adjustable volume mechanical pipette into the quartz glass cuvette, and then a 100 µL chemical agent solution of NaClO was injected into the cuvette by a syringe. CL

signals produced from the cuvette were recorded by a computer equipped with BPCL software, by which data were obtained and processed. In Fig. 1B, PTFE (polytetrafluoroethylene) tubing (0.8 mm i.d.) was used as connector in the flow system. There were two peristaltic pumps, P_1 and P_2, used to deliver all flow solutions. Pump P_1 was used to deliver the flow streams of solution of NaClO, and the other one was used to deliver the carrier water and solution of H_2O_2. By a valve injector with a 100 μL sample loop, aqueous colloid solutions of QDs was injected into the carrier once a time during each sample analysis. A flow cell, made up with a flat spiral-coiled colorless glass tube (1.0 mm i.d.; total diameter of the flow cell, 3 cm, without gaps between loops), was placed closely to the photomultiplier tube (PMT) window. Solutions of NaClO and the mixture of H_2O_2 and aqueous colloid solutions of QDs were pumped into the flow cell, and then they were mixed and reacted in it. The CL signals produced from the reaction were collected and amplified in real-time by a flow CL analyzer (Lumiflow LF-800, Microtec NITI-ON, Funabashi, Japan). Data acquisition and treatment were performed with chromatogram acquisition unit and chromatogram workstation system (HW-2000, Qianpu Software Co., LTD, Shanghai, China). The signals produced by the CL reaction without aqueous colloid solutions of QDs and sample injection were recorded as blank. The determination of selected analysis was quantified by the increased CL intensity $\Delta I = I_s - I_b$, where I_s was the CL intensity of reaction solution, and I_b was the blank signal. With optimized reaction conditions, the increased CL relative intensity (ΔI) was corresponded to the normal maximum light intensity.

2.4 Synthesis of QDs

Fig. 2 shows the synthesis scheme of the Zn-dots. As reported [84], the solution of $ZnSO_4 \cdot 7H_2O$ (0.5 M, pH=3.0), L-cysteine (0.3 M), $MnCl_2 \cdot 4H_2O$ (0.025 M) were heated to 60 ^oC with insert N_2 protection, then the $Na_2S \cdot 9H_2O$ (0.5 M, pH=13.5) solution was added. The mixture formed by above solutions was kept stirring for 30 min until the precipitate could be re-dissolved slowly. Next, the result was dialyzed for 4 days. Into the resultant mixture, 1 mL of TEOS (crosslinking agent) was added and then the mixture was exposed to ultrasonic vibration for 2 min by an ultrasonicator (KQ-500DB, 500 W, 50 Hz, Kunshan Ultrasonic Device Co., Jiangsu Province, China), after which the dispersion mixture was kept stirring for 24 hours and dialyzed against water for 3 days afterwards. Then the resultant Zn-dots was centrifuged and washed with 40 mL of absolute ethanol two times. Finally, Zn-dots was dried in vacuum and stored in a desiccator. More QDs capped with different reagents or doped with different Mn dosage were also synthesized in the same way to screen the optimum one for the research work.

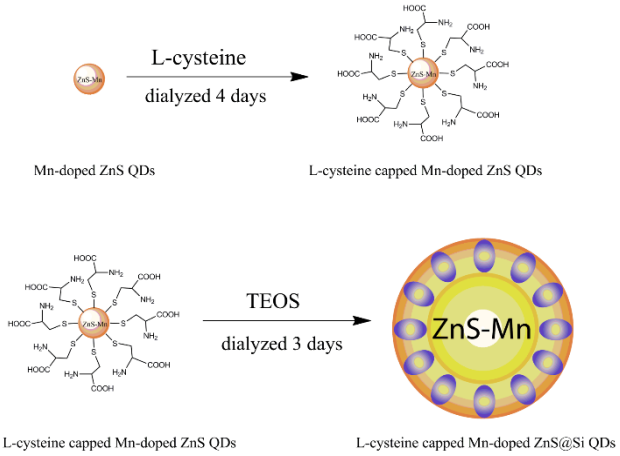

Fig. 2. Schematic illustration for synthesis of Zn-dots.

3 Results and discussion

3.1 Crystalline size and structure

The XRD pattern for Zn-dots was shown in Fig. 3A. The diffraction peaks at 28.8°, 48.85°and 56.05°were corresponded respectively to (111), (220) and (311) planes of the cubic Zinc blende structure, agreeing well with JCPDS No. 1-0792. Fig. 3B showed the TEM images of Zn-dots. In the light of Sherrer's equation, the average crystalline sizes of the samples are about 3.0 nm.

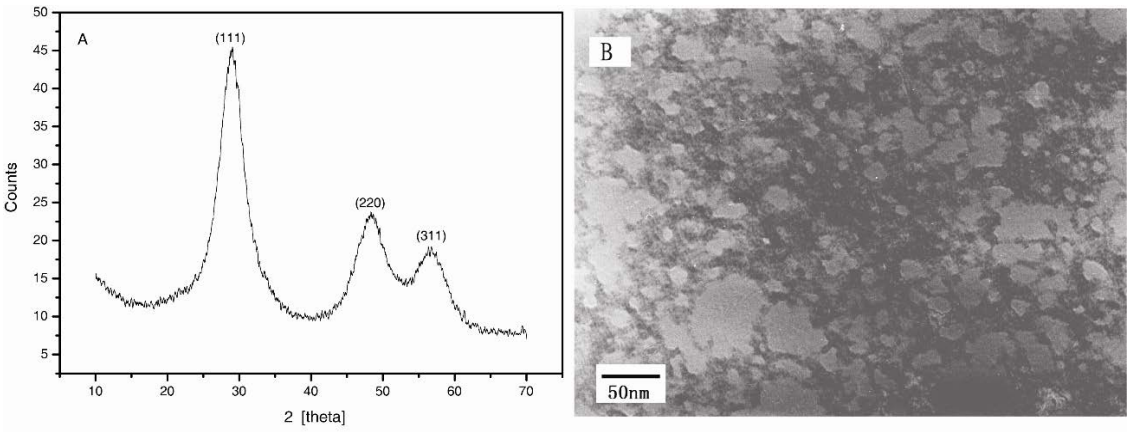

Fig. 3. (A) XRD patterns of L-cysteine capped Mn-doped QDs@Si; (B) TEM pattern of Zn-dots.

3.2. Absorption spectra of QDs

Fig. 4A showed the UV-visible absorption spectra of ZnS@Si QDs, L-cysteine capped ZnS@Si QDs, Zn-dots, L-cysteine capped ZnS QDs and L-cysteine capped Mn-doped ZnS QDs. As depicted in this figure, the spectra of ZnS@Si QDs showed nothing while the others showed strong absorption peaks at 289 nm. Peculiarly, the Zn-dots showed the maximum absorption peak.

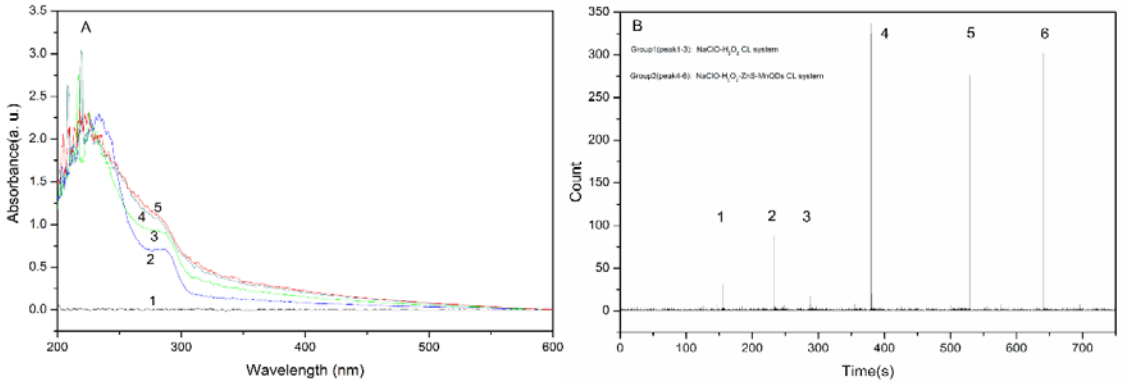

Fig. 4. (A) Absorption spectra of different types of ZnS QDs. 1. ZnS@Si QDs, 2. L-cysteine capped ZnS@Si QDs, 3. L-cysteine capped Mn-doped ZnS QDs, 4. L-cysteine capped ZnS QDs, and 5. Zn-dots; (B) Dynamic CL profiles of NaClO-H_2O_2. The concentrations of NaClO, H_2O_2 and Zn-dots were 1.0×10^{-3} M, 0.5 M and 20 mg/L respectively. Peak 1-3: NaClO-H_2O_2 CL system; Peak 4-6: Zn-dots CL- system.

3.3. Dynamic profile of CL

Fig. 4B showed the chemiluminescent dynamic profile of Zn-dots CL system. CL signals of NaClO-H_2O_2 CL system without other reagents were recorded as blank signals. A weak luminescence was yielded when the solution of NaClO was injected into the solution of H_2O_2. The CL signals reached its maximum intensity immediately in about a second after the injection, which meant the interaction of ClO^- with H_2O_2 being a very fast CL process. When Zn-dots are injected into the NaClO-H_2O_2 CL system, the average CL intensity was enhanced dramatically from about 90 counts to nearly 300 counts, while the CL duration remained almost unchanged.

3.4. CL spectra for the CL system

A series of experiments including concentration optimization of NaClO and H_2O_2 were conducted, and batches of QDs with different dosage of Mn doped and L-cysteine capped were synthesized for screening the best one in enhancing the CL signals of NaOCl-H_2O_2 system by static injection anlysis. The results were shown in Fig. 5. It's well-known that without any modification ZnS QDs is insoluble in water. But after modification with L-cysteine and TEOS, it was found that ZnS QDs were not only soluble in water but also could enhance the CL intensity of NaOCl-H_2O_2 system by nearly 7 folds, and more enhancements could be observed after modified ZnS QDs were doped with Mn according to Figure c compared with a and b in Figure 5. As a transition metal ion, Mn^{2+} incorporated into the ZnS host lattice which catalytically enhanced the CL intensity NaOCl-H_2O_2 system [84]. The amino acid L-cysteine has an thiolate substituent on the side chain of it. The thiol side chain often participates in enzymatic reactions, serving as a nucleophile. Beyond the iron-sulfur proteins, many other metal cofactors in enzymes are bound to the thiolate substituent of cysteinyl residues. In this paper, the thiolate substituent of L-cysteine serves as a nucleophile bounding to the Mn doped in the QDs; the other parts of L-cysteine are hydrophilic, which facilitate the modified QDs to become soluble in water. According to Fig. 5D, the CL signal is increased in early range of dosage of L-cysteine, which originates from the increased mounts of soluble QDs after it is modified with increased mounts of L-cysteine. But when the dosage of L-cysteine is over 4.2% (mass %), the CL signal is decreased. It's probably due

the surface of ZnS@Si QDs are overcovered with L-cysteine which preventing the interaction between active-species of NaOCl-H_2O_2 system and ZnS@Si QDs. Also the effect of NaN_3 on CL-emission signal with reaction systems were investigated and the results shows that when NaN_3 is added to NaOCl (inset a), H_2O_2 (inset b), and L-Cysteine (capped)-Mn(doped)ZnS@Si QDs (inset c), there are no CL signals detectable, which means NaN_3 have no effect on them.

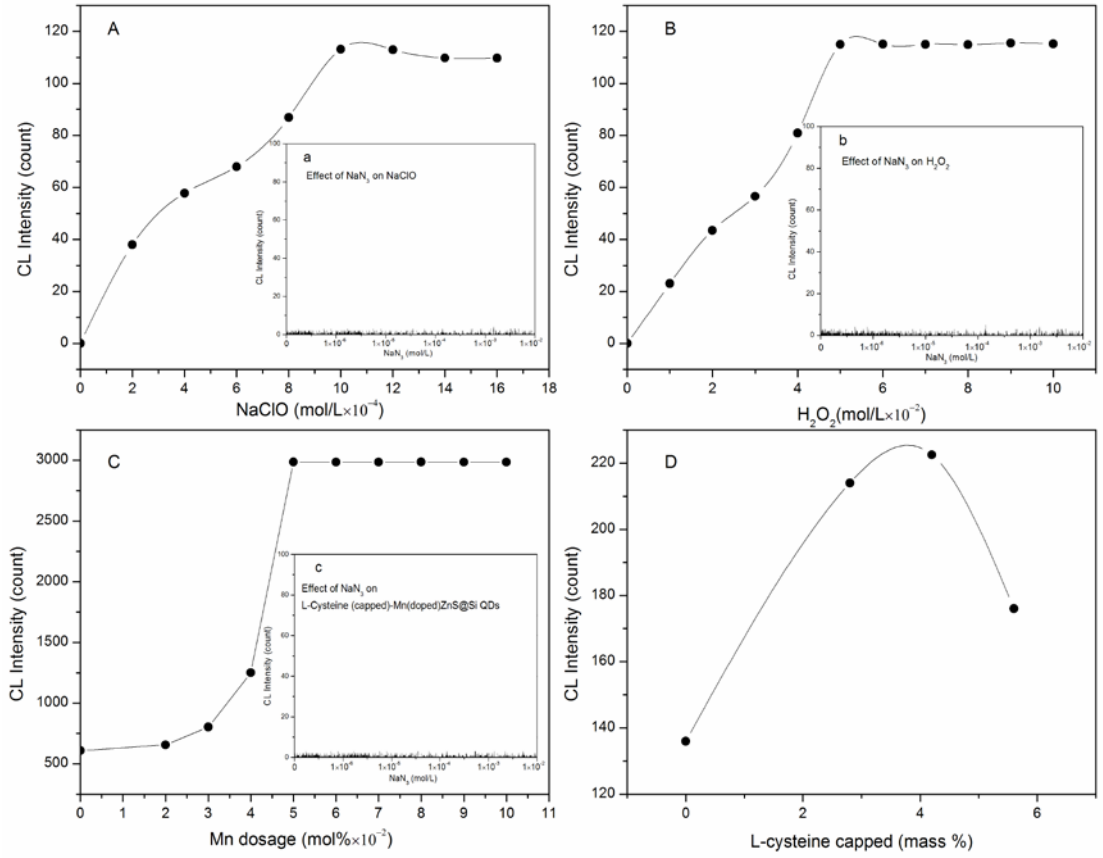

Fig. 5. Optimization of the experimental conditions. (A) Effects of NaClO concentration: 5.0×10^{-2} M H_2O_2; (B) Effects of H_2O_2 concentration: 1.0×10^{-3} M NaClO; (C) Effect of dosages of Mn doped in the ZnS@Si QDs: 5.0×10^{-2} M H_2O_2, 1.0×10^{-3} M NaClO; (D) Effect of dosages of L-cysteine capped to the ZnS@Si QDs: 5.0×10^{-2} M H_2O_2, 1.0×10^{-3} M NaClO.

Considering the CL intensity and the consumption of the reagents, the optimized conditions for the CL system were as follows: 1.0×10^{-3} M NaClO,

5.0×10^{-2} M H_2O_2, 5% (mole %) Mn doped and 4.2% (mass %) Zn-dots used as synthesized; the optimum rates of two flows were at the same of 2.6 mL/min and the shortest possible length of mixing tube was preferable. Under the optimized conditions, the CL response of the Zn-dots to the NaClO-H_2O_2 CL system was investigated (Fig. 6). It was found that, with the concentration increase of Zn-dots from 0.08 mg/L to 50 mg/L, the CL intensity increased correspondingly from an average of 0.26 mV (part c, about twice the blank signal of part b) to average 4.5 mV (part g, about 23 times as high as the blank signal of part b). The CL intensity shown a linear correlation relationship with the concentration of the Zn-dots. On the other hand, the illumination duration of each interaction of Zn-dots with CL system was nearly the same of about 0.3 min.

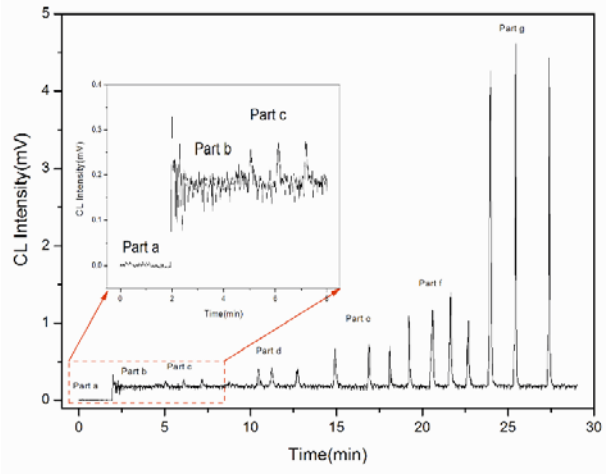

Fig. 6. CL profile of the Zn-dots-NaClO-H_2O_2 CL system. concentrations of aqueous colloid solutions of QDs (part c to part g): 0.08, 0.4, 2, 10, 50 mg/L; H_2O_2: 5.0×10^{-2} M; NaClO: 1.0×10^{-3} M; work condition: flow rate, 2.5 mL/min.

3.5. Quenching effect on the CL system

A well-known quencher of $^1O_2$, NaN_3 was used in this experiment [85]. Fig.

7 shows the effective quench of NaN_3 on the CL system. It was found that with the increasing of concentration of NaN_3 from 1.0×10^{-7} to 1.0×10^{-3} M, the CL intensity was decreased from about 475 counts to nearly zero. The results proved adequately the generation of $^1O_2$ during CL reactions. To further confirm the existence of $^1O_2$ in the CL reaction, electron spin resonance (ESR) spin trapping technique was employed.

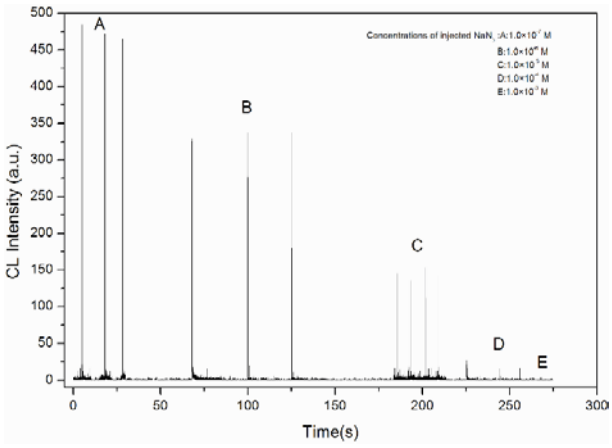

Fig. 7. Effect of NaN_3 on the CL signals. Batch method: 50 μL of 1.0×10^{-3} M NaClO solution was injected into 50 μL of 5.0×10^{-2} M H_2O_2 solution pre-mixed with NaN_3. Concentrations of NaN_3 were 1.0×10^{-3} M, 1.0×10^{-4} M, 1.0×10^{-5} M, 1.0×10^{-6} M, and 1.0×10^{-7} M, respectively.

3.6. ESR spin-trapping with 5, 5-dimethyl-1-pyrroline-N-oxide and 2, 2, 6, 6-tetramethyl 1-4-piperidine

5, 5-Dimethyl-1-pyrroline-N-oxide (DMPO) and 6, 6-tetramethyl 1-4-piperidine (TEMP) were used as spin-trapping agents for the detection of hydroxyl radical and singlet oxygen respectively. Fig. 8 shows the specific signals of DMPO-OH and TEMPO, which were produced by the reaction of spin-trapping agents with NaClO and H_2O_2 (Schemes 1 and 2).

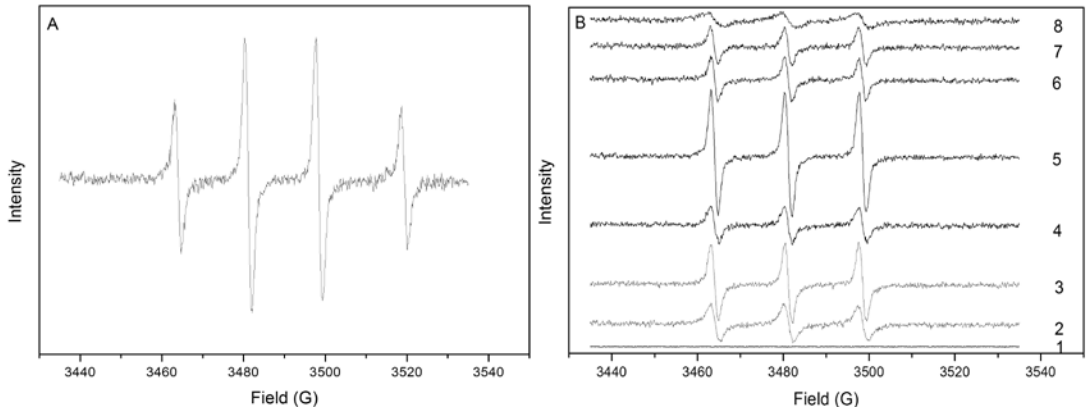

Fig. 8. (A) ESR spectra of the DMPO adduct with $^{\bullet}OH$ generated in Zn-dots-NaClO-H_2O_2 CL system; (B) ESR spectra of TEMPO by reaction of TEMP with singlet oxygen generated in Zn-dots-NaClO-H_2O_2 CL system: (1) H_2O (blank); (2) H_2O_2-NaClO; (3) H_2O_2-NaClO-ZnS@Si QDs; (4) H_2O_2-NaClO with addition of 1.0×10^{-6} M NaN_3; (5) Zn-dots-NaClO-H_2O_2; (6)-(8) Zn-dots-NaClO-H_2O_2 with addition of increased concentration of NaN_3 (1.0×10^{-6} M, 1.0×10^{-5} M, and 1.0×10^{-4} M); Conditions: receiver gain=8.00e+04; Modulation amplitude=1.04 G; Sweep width=100.00 G; Microwave frequency=9.7500 GHz.

Scheme 1. DMPO-OH formation from NaOCl and H_2O_2

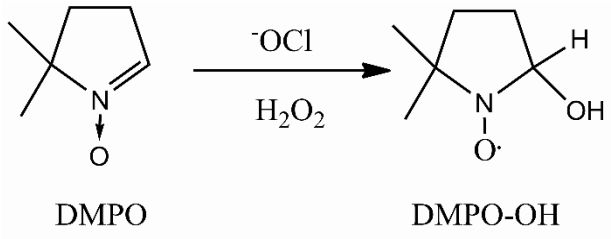

Scheme 2. TEMPO formation from $^1O_2$

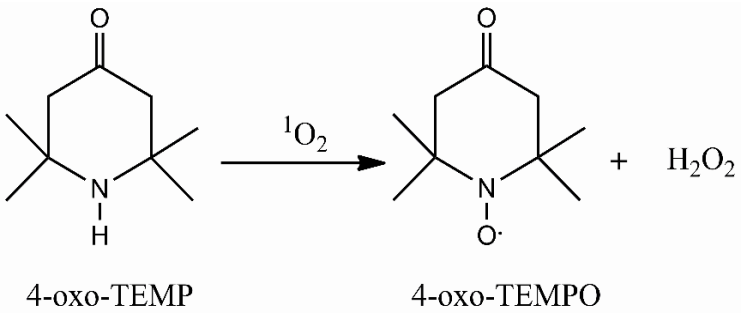

The results in Fig. 8A indicated the formation of $^{\bullet}OH$, which, in alkaline conditions, generated through an electron transfer process between ^{-}OCl and H_2O_2 as shown in Eq. 1 (Scheme 3). According to the Marcus theory [86], an outer sphere electron transfer was possible when the donor standard oxidation potential (E_{ox}) minus the acceptor standard reduction potential (E_{red}) was lower than 0.4 V. To E_{ox} of ClO_2^- (0.69 V *vs* NHE, involving two electrons), the E_{ox} of ClO^- was lower than 0.69 V *vs* NHE, and the E_{red} ($H_2O_2/^{\bullet}OH$, ^{-}OH) was 0.32v *vs* NHE, which meant that the potential difference (ΔE) between E_{ox} ($ClO^-/ClO^{\bullet}$) and E_{red} ($H_2O_2/^{\bullet}OH$, ^{-}OH) was lower than 0.37 V and an electron transfer process between ^{-}OCl and H_2O_2 as shown in Equation 1 was possible according to the Marcus theory.

Fig. 8B showed the specific signals of TEMPO. Among the spectra 1-8 of Fig. 8B, Spectrum 2 indicated the generation of singlet oxygen in the NaClO-H_2O_2 CL system. Spectrum 3 showed the enhanced signals of NaClO-H_2O_2 CL system after the ZnS@Si QDs was added into it. And the enhancement exhibited more when ZnS@Si QDs was replaced with Zn-dots being added into the NaClO-H_2O_2 CL system (Spectrum 5). But all the signals in Spectrum 2, 3, and 5 were inhibited after quencher NaN_3 was added into the CL system. Moreover, the quench effect increased with the increasing concentration of NaN_3 from 1.0×10^{-7} to 1.0×10^{-3} M (Spectrum 4, 6, 7, and 8 of Fig. 8B). The results indicated firmly that the singlet oxygen was formed during the CL reactions.

The UV and ESR spectra of QDs before and after modified with Mn-doped

(Fig. 5C) and L-cysteine capped (Fig. 5D) demonstrated a strong molecular interaction within ZnS@Si QDs, the capping layer and the element doped. The carboxyl and amino group of the L-cysteine at the outer surface of Mn-doped ZnS@Si QDs behaved as the receptor sites through the acid-base pairing interaction, which was very important in the CL energy transfer process. Moreover, with unsaturated valence electrons $3d^5$ and the activity effect of transition element manganese, Zn-dots acted as the catalytic center and made faster the decomposition of H_2O_2 with the generation of intermediates of $^{\bullet}OH$ and $O_2^{\bullet-}$ (Eq. 3). The superoxide anion $O_2^{\bullet-}$ was active and could interact with the intermediate of $^{\bullet}OH$ forming $^1O_2$ (Eq. 4). In addition, as shown in Equation 5, the intermediates radicals $^{\bullet}OH$ and $ClO^{\bullet}$ might couple together to form HO_2Cl, which further decomposed, in basic medium, to yield monomol $^1O_2$ (Eq. 6). $^1O_2$, on the other hand, was also active and easy to form excited $(^1O_2)_2^*$, a dimer aggregate of monomol singlet oxygen. This dimer, by an energy transfer process, was very easy to transfer its energy to Zn-dots forming excited QDs (Eq. 8).

Therefore, according to the discussions above, the CL mechanism of the sensitized NaClO-H_2O_2 CL system induced by Zn-dots could be summarized as the following expressions (Scheme 3). In alkaline conditions, ClO^- interacted with H_2O_2 producing the radicals $^{\bullet}OH$ and $ClO^{\bullet}$ (Eq. 1); H_2O_2 could also reacted with ^-OH forming HO_2^- (Eq. 2). When NaClO-H_2O_2 CL was induced by the sensitizer, the decomposition of H_2O_2 was catalyzed to generate intermediates radicals $^{\bullet}OH$ and $O_2^{\bullet-}$ (Eq. 3). Then the intermediate superoxide

anion interacted with the intermediate $^{\bullet}OH$ with the generation of singlet oxygen ($^1O_2$) (Eq. 4); also, the intermediates radicals $^{\bullet}OH$ and $ClO^{\bullet}$ might couple together to form HO_2Cl (Eq. 5), which further decomposed, in basic medium, to yield monomol $^1O_2$ (Eq. 6). An excited dimer $(^1O_2)_2^*$ was then formed and CL emission was then observed when $(^1O_2)_2^*$ returned to its ground state (Eq. 7). We suggested that a CL resonance energy transfer process also occurred between the donors $(^1O_2)_2^*$ and the acceptors Zn-dots to from an excited QDs (Eq. 8). Finally, the enhanced CL signals were observed while the excited QDs returned to its ground state (Eq. 9).

Scheme 3: Suggested CL mechanism for Zn-dots -NaClO-H_2O_2 CL system

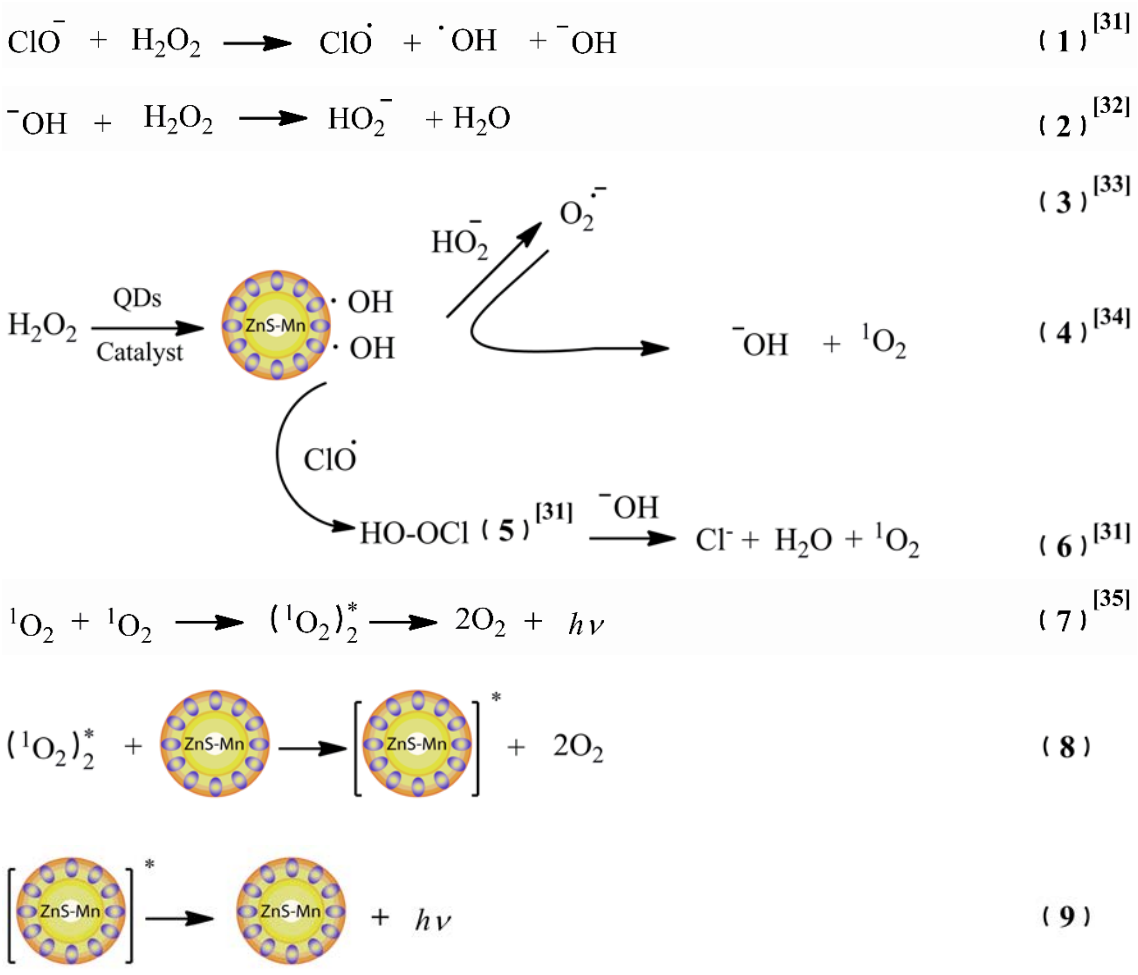

4 Conclusions

In summary, the weak CL system of NaClO-H_2O_2 could be sensitized when it was induced by the sensitizer of Zn-dots. This sensitizer acted as an efficient catalysis center and an energy acceptor in CL resonance energy transfer process. In the presence of sensitizer, the decomposition of H_2O_2 and the formation of monomol singlet oxygen ($^1O_2$) and excited dimol $(^1O_2)_2^*$ were promoted in the NaClO-H_2O_2 CL reactions; an energy transfer process occurred between donor of excited dimol singlet oxygen $(^1O_2)_2^*$ and acceptor of sensitizer. The CL signals of the NaClO-H_2O_2 system were finally enhanced dramatically by the sensitizer in the whole. This work was important for investigation of new and efficient catalysts of CL system and helpful for comprehension of CL mechanism correspondingly.

Chapter 4 Carbon nanodots sensitized chemiluminescence on

peroxomonosulfate–sulfite–hydrochloric acid system and its analytical application

1 Introduction

Recently, C-dots have been paid great attention in many fields [87-91]. They are discrete and almost spherical nanoparticles with sizes below 10 nm. They can be bought inexpensively and easily in bulk by many methods (for example, electrochemical oxidation of graphite or multiwalled carbon nanotubes, one-step pathway of microwave pyrolysis approach, etc.) [92-99]. They have many luminescent properties such as strong optical absorption in the UV region [100-102], photoluminescence produced with photoexcitation [103-105], and electrochemiluminescence (ECL) generated by electron injection [106]. They have many other amazing characteristics: size and wavelength-dependent luminescence emission, resistance to photobleaching, and ease of bioconjugation without toxicity and environmental hazard. Besides these outstanding advantages, the most commendable is that they are covered with hydrophilic hydroxyl of PEG 200 covered outside. Therefore they have good solublility in water, which greatly deepens their applications as many reactions occurring in aqueous phase systems [107-112].

Water soluble aliphatic primary amines (i.e. C1: methylamine, C2: ethylamine, C3: n-propylamine, C4: n-butylamine, and C5: n-pentylamine) are degradation products of biological systems, such as amino acids and proteins. They are widely distributed in the environment as the byproducts of industrial

and agricultural activities. Residues of these amines are hazardous to human health due to their pungent and irritant odor to skin, eyes, etc. [113-115] But in some environmental water, the quantities of aliphatic primary amines are too small to be detected. Thus, a rapid and sensitive technique for the detection of aliphatic primary amines in water samples is very necessary.

CL technique is a cheap and simple optical detection system. It has low background noise, low detection limit, and wide working range [116-119]. It has been proven effective in rapid and sensitive measurements at ultra-trace levels. Recently, CL detection technique incorporates widely with C-dots in many CL systems, which broadens its application fields [120-124].

In this paper, water-soluble C-dots were prepared easily in a facile microwave pyrolysis approach in minutes. Incorporated with these C-dots, a novel potassium peroxymonosulfate – sodium sulfite -hydrochloric acid (PSHA) CL system was developed. It consists of C-dots, sulfite, hydrochloric acid and peroxomonosulphate ($KHSO_5$). $KHSO_5$ is an inexpensive, commercially available potassium carotate. It acts as a provider of excited singlet oxygen ($^1O_2$) in many CL systems [125-127]. Investigation indicated that C-dots had apparent sensitization effects on PHSA CL system. Possible mechanism of C-dots sensitized PHSA CL system was proposed. Further investigation indicated that the CL enhancements of C-dots could be inhibited by the addition of aliphatic primary amines. This inhibited method exhibited a linear range of 1×10^{-9} to 1×10^{-5} M with detection limits of 2.5×10^{-10} to 3.3×10^{-9} M. The proposed CL system was successfully applied for the determination of aliphatic primary

amines in water samples.

2 Experimental

2.1 Chemicals and materials

Ultra-purification water was prepared with a Compact Ultrapure water system (18.3 MΩ.cm). The analytical reagent-grade chemicals were used throughout. A solution of $KHSO_5$ was prepared daily by dissolving a triple salt (K_2SO_4•$KHSO_4$•$2KHSO_5$, Alfa, Ward Hill, USA) in water. Na_2SO_3 and HCl were all from Tianjin Kaitong Chemicals Co. (Tianjin, China). They were also prepared daily. PEG 200 and glycerol were obtained from Shantou Xilong Chemical Factory (Guangdong, China). Glycine (assay≥99%) was from Dingguo Changsheng Biotechnology Co., Ltd. (Beijing, China). Aliphatic primary amines (i.e. methylamine, assay 30～33%; ethylamine, assay 65～70%; n-propylamine, assay≥98.5%; n-butylamine, assay≥99%; and n-pentylamine, assay≥97%) were from Sigma-Aldrich Co. (USA).

2.2 Apparatus

C-dots were synthesized within an 800 W microwave oven (Galanz G8023CSL-K3, Galanz Group, Guandong, China). Static CL measurements were performed with an ultra-weak CL analyzer (Institute of Biophysics, Chinese Academy of Science, Beijing, China). A flow CL analyzer (Lumiflow LF-800, Microtech NITI-ON, Funabashi, Japan) was used in flow injection CL measurements. PL spectra were examined by F-7000 fluorescence spectrophotometer (Hitachi, Japan). UV-vis absorption spectra were achieved

with a Model UV-2100s Spectrophotometer (Shimadzu, Japan). Particle sizes and morphologies of C-dots were measured by a transmission electron microscope (TEM, Tecnai G^2 20 S-Twin, FEI Company, USA) at 200 kV. The TEM samples were prepared by casting a drop of C-dots solution in nanopure water onto a 300-mesh holey carbon-coated copper grid for observation. ^{13}C NMR spectra were collected with a JNM-ECX 400 MHz spectrometer (JEOL LTD, Japan) by dissolving 30 mg of C-dots in 0.5 mL deuterated water. Ultrasonic instrument (KQ-500DB, 500 W, Kun Shan Ultrasonic Instruments Co., Ltd) was used for mixing solutions well.

2.3 Synthesis of C-dots

C-dots were synthesized according to Ref. [96] with little modification. Briefly, PEG 200 (1 mL) and glycine (1 mM) were added into glycerin (5 mL). Then they were mixed well by an ultrasonic instrument. Next, the mixture was heated for 6 min in a microwave oven. Increasingly, the color of the heated solution changed from colorless to dark brown. Then the result was dialyzed for 4 days. Finally, a light green result was prepared and labeled as C-dots. It was then dried in a vacuum rotary evaporator and stored in a refrigerator at 4 ℃ for future use (Fig. 1).

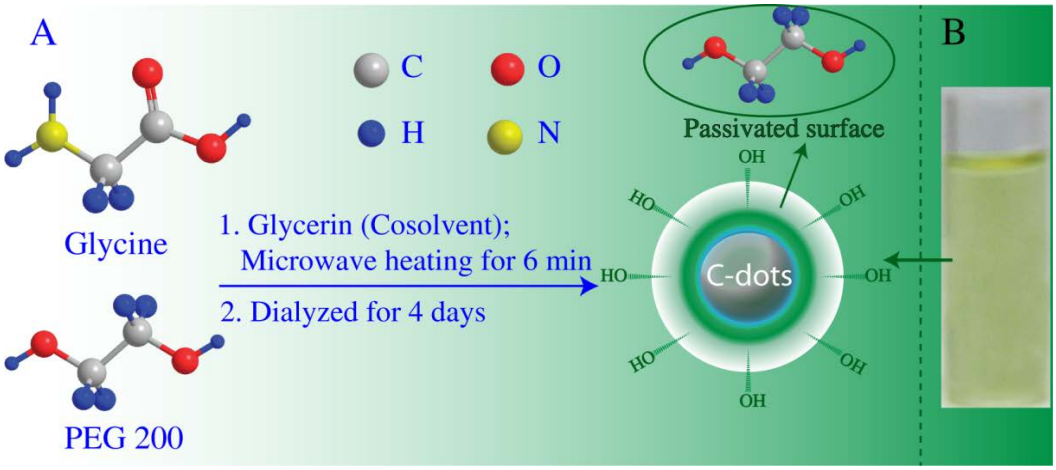

Fig. 1. (A) Schematic illustration for the synthesis of C-dots and (B) photo of light green results after been dialyzed for 4 days.

2.4 Procedure for PSHA dynamic CL

To investigate the dynamic properties of PSHA CL system, static injection CL analysis was carried out in a 3 mL quartz glass cuvette by a batch method. Every time before static CL measurement was taken, the analyzer ran for 10 min in order to obtain good mechanical and thermal stability. After that, a solution of Na_2SO_3 (100 µL) was added to the mixture of $KHSO_5$ (100 µL) and C-dots (100 µL) in the cuvette. Immediately, a solution of HCl (100 µL) was injected into it too. The CL intensity was displayed and integrated instantly with the luminescence analyzer. The analyzer ran at a 0.01 s sample interval and -1.2 kV PMT work voltage.

2.5 Procedure for PSHA CL

A flow injection analysis (FIA) was employed to perform the C-dots sensitized PSHA CL system (Fig. 2). Two peristaltic pumps were used to deliver four flowing streams in this FIA method. PTFE (polytetrafluoroethylene) tubing

(0.8 mm i.d.) was used as the delivery channel. The sample injection part was a six way valve which was equipped with a 100 µL sample loop. A spiral flow cell made of organic glass with an inner diameter of about 1 mm was placed on the top window of a photomultiplier tube (PMT, Hamamatsu, Japan). PMT was used as a detector of CL signals. Prior to running, the FIA instrument was rinsed out thoroughly for about 20 min to get a stable baseline record. The flow rates of all lines were set as 1 mL min^{-1}. In a sample injection procedure, 100 µL Na_2SO_3 solution was injected into a carrier stream, and then mixed with the mixture formed from other three lines: C-dots, HCl, and $KHSO_5$. The final mixture then reached the flow cell and immediately produced CL emission. Distance between the final mixing point and flow cell was about 5 cm. The produced CL signal was detected and recorded by a computerized flow CL analyzer. Data acquisition and treatment were performed with Lumiflow software which ran under Windows XP system.

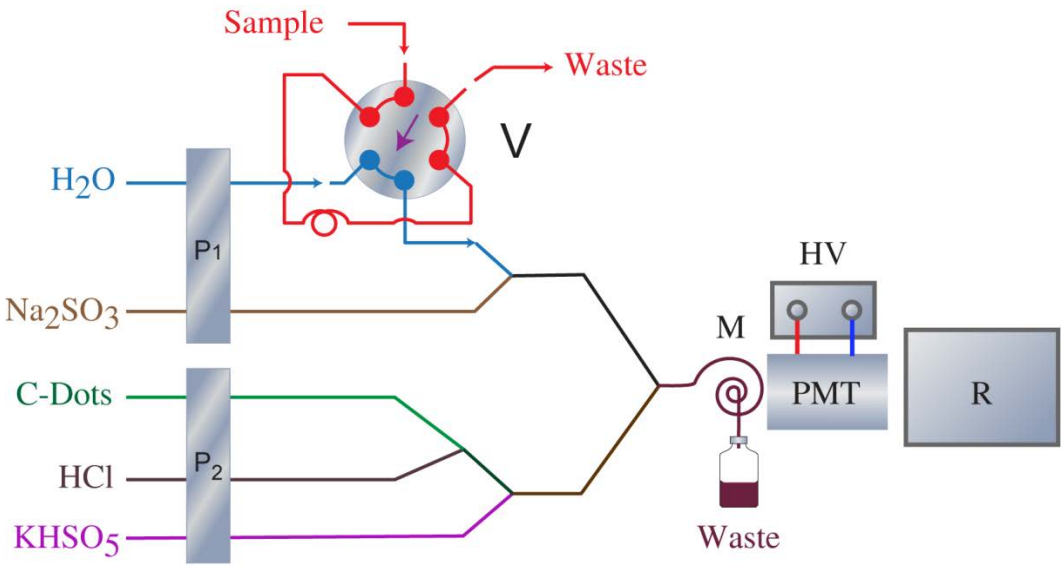

Fig. 2. Schematic diagram of FIA CL system. P_1 and P_2, peristaltic pump; V,

six-way injection valve; M, CL flow cell; W, waste; HV, negative high-voltage power supply; PMT, photomultiplier tube detector; R, luminescence analyzer controlled by personal computer.

2.6 Procedure for inhibited CL detection of aliphatic primary amines

Fig. 2 depicts the lab-built FIA CL detection system. In scheduled procedure, the flow rates of the detection system were fed at 1 mL min^{-1}. Firstly, the FIA CL detection system was washed well until a stable baseline signal was achieved. A 100 μL sample solution was injected into the carrier stream and then mixed with Na_2SO_3 solution. Finally, all carried solutions merged and flowed into a flow cell, accompanying with an inhibited CL signal. The concentration of samples was quantified by the relative decreased CL intensity.

3 Results and discussion

3.1 Characterization of C-dots

The UV-vis absorption spectra and PL spectra of six synthesized C-dots under different microwave heating time were shown in Fig. 3A and B, respectively. The spectra c and d in Fig. 3A displayed strong absorptions of C-dots at about 470 nm, while the others shown almost no (a and f) or weak absorptions (b and e). The C-dots (c) were then selected as the sensitizer of PHSA CL system. Fig. 3B displayed the PL spectra of the selected C-dots with a maximum emission of around 502 nm. Based on the facts above, it’s suggested that under short microwave heating time (less than 6 min) C-dots were not shaped well or only small parts were shaped (showing weak or no absorption in UV spectra, as

shown in spectra a and b of Fig. 3A). But the longer microwave heating time (more than 8 min) C-dots underwent, the less absorption the C-dots had (spectra e and f of Fig. 3A). This was probably due to the carbonation of nanocrystalline core of C-dots and PEG 200. Usually, C-dots had high activities in solution with passivation layers of PEG 200 covering outside. After being heated for a long time, the carbonation of C-dots and PEG 200 damaged the structure and thus caused the loss of activities of the C-dots.

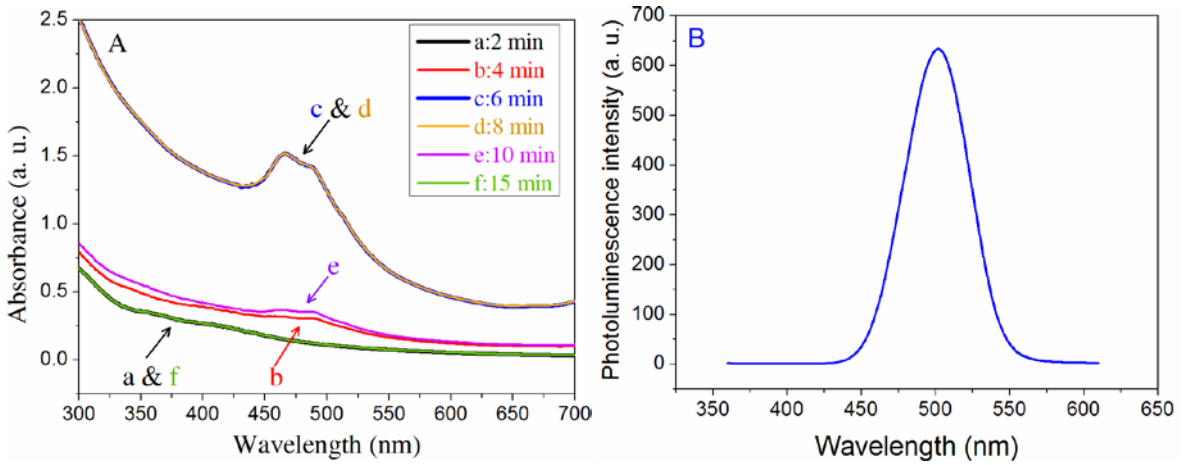

Fig. 3. Optical property of C-dots: (A) Absorption spectra of C-dots synthesized under different microwave heating time; a to f: 2 to 15 min of microwave heating time. Spectra a and f, c and d almost overlapped each other; (B) PL spectra of selected C-dots synthesized under 6 min of microwave heating time, excitation wavelength: 470 nm.

^{13}CNMR spectra of the C-dots were shown in Fig. 4A. The peaks below 80 ppm arose from PEG 200, the outside passivation layer of C-dots. In detail, the peaks at 61.5 and 72.8 ppm (Fig. 4A) were attributed to terminal α and β C (sp^3) of PEG 200; the peak at 70.5 (Fig. 4 A) was assigned to the methylene carbon

(sp^3) of the main chain [128]. The peaks centered at 135 ppm (Fig. 4 A) were ascribed to the polycyclic carbons (sp^2) of the C-dots [91]. Thus, C-dots consisted most probably of nanocrystalline cores with graphitic carbons (sp^2) inside and PEG 200 with hydrophilic functional groups of hydroxyl outside. These outward groups enabled C-dots had a good water-solubility and wide applications. The inset of Fig. 4A displayed the TEM images of C-dots. The particles of C-dots were mostly of spherical and dispersed rather evenly on the surface of the TEM copper grid, with sizes averaging about 3.0 nm.

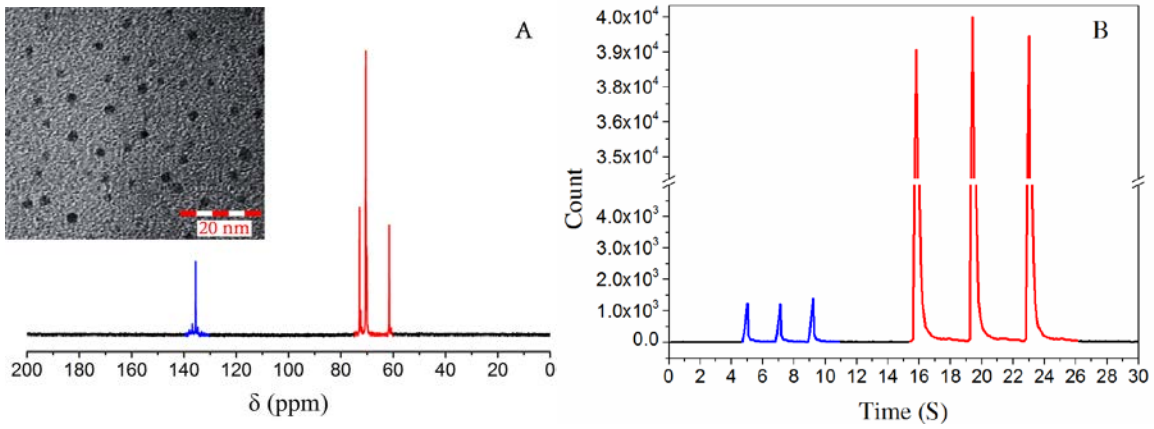

Fig. 4. ^{13}CNMR spectra of C-dots in D_2O; Inset: TEM pattern of C-dots (A) and Dynamic profiles for PHSA CL system with and without C-dots (B). Blue peaks in profile B: 100 μL 1×10^{-2} M Na_2SO_3 solutions was injected firstly into a mixture of 100 μL 1×10^{-2} M $KHSO_5$ solution and 100 μL water, and then 100 μL 1×10^{-2} M HCl solution was injected as quickly as possible; Red peaks in profile B: 100 μL 1×10^{-2} M Na_2SO_3 solutions was injected firstly into a mixture of 100 μL 1×10^{-2} M $KHSO_5$ and 100 μL 4×10^{-5} M C-dots solutions, and then 100 μL 1×10^{-2} M HCl solution was injected as soon as possible; High voltage, -1.1 KV; Sample interval, 0.1s.

3.2 Dynamic CL profiles of the PSHA CL

The dynamic profiles of PHSA with and without C-dots sensitized CL systems were acquired in static injection analysis. Results demonstrated that the CL reactions were very quick (Fig. 4B). After the CL reaction began, the CL intensity reached a maximum up to 1247 counts at about 2s for PHSA system (Fig. 4B) and 40508 counts at about 3.5 s for PHSA-C-dots system (Fig. 4B). Obviously, the CL intensity of PHSA-C-dots system was far stronger (about 33 times) than that of the PHSA system. The C-dots showed great sensitization effects on the PHSA CL system.

3.3 FIA CL profile of the PSHA CL system before and after being sensitized by C-dots

Concentrations of PHSA-C-dots CL system were then systematically investigated to achieve optimal conditions (Table 1). The best concentration of C-dots was at 4×10^{-5} M. And the concentrations of $KHSO_5$, Na_2SO_3 and HCl were at 1×10^{-2} M, respectively. Under the optimal conditions, the FIA CL profile of PSHA CL system before (Fig. 5A) and after (Fig. 5B) being sensitized by C-dots was obtained. Results in Fig. 5 displayed great sensitized enhancement effects of the C-dots on the PSHA CL system. The running mode of FIA CL analysis was shown in Fig. 2.

Table 1. Optimization of the reaction concentrations

$KHSO_5$		Na_2SO_3		HCl		C-dots	
Concn (M)	CL intensity (count)	Concn (M)	CL intensity (count)	Concn (M)	CL intensity (count)	Concn (M)	CL intensity (count)
1×10^{-5}	1.3×10^{3}	1×10^{-5}	1.2×10^{3}	1×10^{-5}	1.4×10^{3}	4×10^{-6}	1.1×10^{3}
1×10^{-4}	16.7×10^{3}	1×10^{-4}	15.3×10^{3}	1×10^{-4}	18.9×10^{3}	4×10^{-5}	12.2×10^{3}
1×10^{-3}	27.1×10^{3}	1×10^{-3}	26.4×10^{3}	1×10^{-3}	28.3×10^{3}	4×10^{-4}	30.7×10^{3}
1×10^{-2}	39.3×10^{3}	1×10^{-2}	39.1×10^{3}	1×10^{-2}	39.7×10^{3}	4×10^{-3}	40.5×10^{3}
1×10^{-1}	39.4×10^{3}	1×10^{-1}	39.2×10^{3}	1×10^{-1}	39.6×10^{3}	4×10^{-2}	40.3×10^{3}

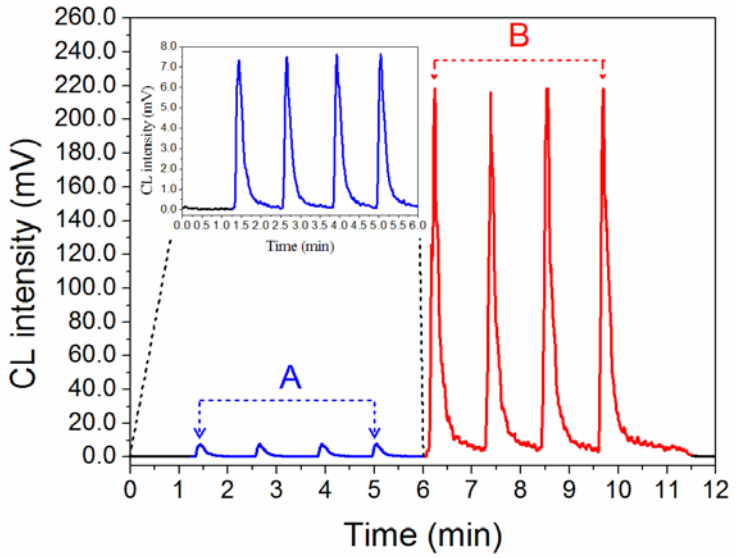

Fig. 5. FIA CL profile of the PSHA CL system before (Blue peaks in group A) and after (Red peaks in group B) being sensitized by C-dots. Solutions of $KHSO_5$, Na_2SO_3 and HCl were all 1×10^{-2} M and the C-dots solution was 4×10^{-5} M; Flow rate : 1 mL min^{-1}; High voltage, -0.8 KV.

3.4 Interferences

The influence of common ions was studied by preparing solutions containing C1 (1×10^{-7} M). The tolerable concentration ratios for interference level at 5% were over 1000- fold for Na^{+}, Ca^{2+}, Mg^{2+}, CO_3^{2-},SO_4^{2-}, 100- fold for K^{+}, Fe^{3+},

NO_3^-, Cl^-, and 10-fold for Cu^{2+}, NH_4^+, $H_2PO_4^-$, respectively. Most ions caused no interferences at the concentrations of lower than 1×10^{-4} M. Ions such as CO_3^{2-}, NH_4^+ at the concentrations higher than 1×10^{-4} M had negative effects thanks to their influence on the pH value of the CL system.

3.1. Possible mechanism of C-dots enhanced CL reaction

$KHSO_5$ is a powerful organic oxidant under acidic conditions [125]. In the present system, HSO_5^- was acidified firstly to form peroxymonosulphurous acid H_2SO_5 (Reaction 1). H_2SO_5 was unstable and very apt to decompose to hydroxyl radical (HO•) and bisulfite radical (HSO_4•) (Reaction 2). Next, hydroxyl radical (HO•) combined itself to form hydrogen peroxide (H_2O_2) (Reaction 3) [129].

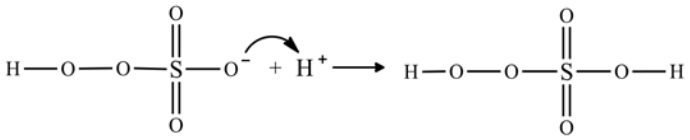

(1)

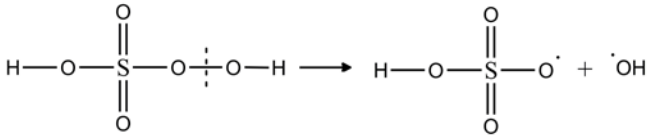

(2)

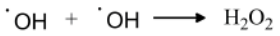

(3)

In addition, sulfite (SO_3^{2-}) was also acidified to form bisulfite ion (HSO_3^-) (Reaction 4). HSO_3^- was further oxidized by hydrogen peroxide (H_2O_2) to produce HSO_3• (Reactions 5 and 6) [130, 131]. Two HSO_3• radicals combined immediately to generate $S_2O_6^{2-}$ which finally decomposed to generate an excited intermediate SO_2^* (Reactions 7 and 8) [132].

(4)

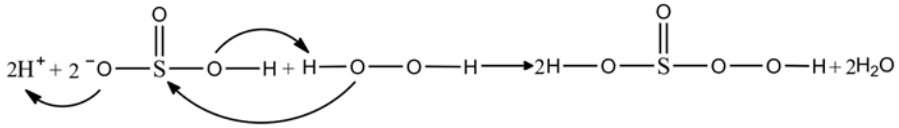

(5)

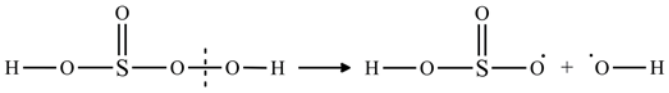

(6)

$$2HSO_3^{\cdot} \longrightarrow S_2O_6^{2-} + 2H^+ \quad (7)$$

$$S_2O_6^{2-} \longrightarrow SO_4^{2-} + SO_2^{*} \quad (8)$$

SO_2^{*} is an important intermediate. It has a wide emission spectra range of 450-600 nm [133]. This range overlapped well with the absorption band and the excitation wavelength of the sensitizer C-dots (Fig. 3A and B). Therefore, the excited SO_2^{*} could pass its energy to the sensitizer C-dots. And a CL resonance energy transfer occurred between SO_2^{*} (donors) and acceptors (C-dots) (Reaction 9). The excited C-dots (C-dots*) finally returned to their ground states with producing of CL emissions (Reaction 10) [134].

$$SO_2^{*} + \text{C-dots} \longrightarrow SO_2 + \text{C-dots}^{*} \quad (9)$$

$$\text{C-dots}^{*} \longrightarrow \text{C-dots} + h\nu \quad (10)$$

At the same time, H_2O_2 reacted with $^{\cdot}OH$ to form $HO_2^{\cdot}$ (Reaction 11) [133]. $HO_2^{\cdot}$ was unstable. It decomposed to intermediate radicals H^+ and $O_2^{\cdot -}$ (Reaction 12) [134]. These intermediate radicals further reacted with C-dots to produce C-dots$^{\cdot +}$ and C-dots$^{\cdot -}$ by the processes of hole and electron injection (Reactions 13 and 14). C-dots in excited state were then formed by electron-transfer annihilation processes between C-dots$^{\cdot +}$ and C-dots$^{\cdot -}$ (Reaction 15) [134].

$$^{\cdot}OH + H_2O_2 \longrightarrow HO_2^{\cdot} + H_2O \quad (11)$$

$$HO_2^{\cdot} \longrightarrow H^+ + O_2^{\cdot -} \quad (12)$$

$$^{\cdot}OH + \text{C-dots} \longrightarrow {}^{-}OH + \text{C-dots}^{\cdot +} \quad (13)$$

$$O_2^{\cdot -} + \text{C-dots} \longrightarrow O_2 + \text{C-dots}^{\cdot -} \quad (14)$$

$$\text{C-dots}^{\bullet+} + \text{C-dots}^{\bullet-} \longrightarrow \text{C-dots}^{*} + \text{C-dots} \quad (15)$$

Also, electron transfer processes occurred between H_2O_2, radical $^{\bullet}OH$ and the intermediate C-dots$^{\bullet-}$ (Reactions 16 and 17) to generate the excited C-dots*, as did the radical $O_2^{\bullet-}$ (Reaction 18). Finally, CL emissions were produced from the return of the excited C-dots* to their ground states (Reaction 10). The main points of the possible CL reaction mechanisms were briefly illustrated in Fig. 6.

$$^{\bullet}OH + \text{C-dots}^{\bullet-} \longrightarrow {}^{-}OH + \text{C-dots}^{*} \quad (16)$$

$$H_2O_2 + \text{C-dots}^{\bullet-} \longrightarrow 2OH^{-} + \text{C-dots}^{*} \quad (17)$$

$$O_2^{\bullet-} + \text{C-dots}^{\bullet+} \longrightarrow O_2 + \text{C-dots}^{*} \quad (18)$$

$$2SO_3^{2-} + O_2 \longrightarrow 2SO_4^{2-} \quad (19)$$

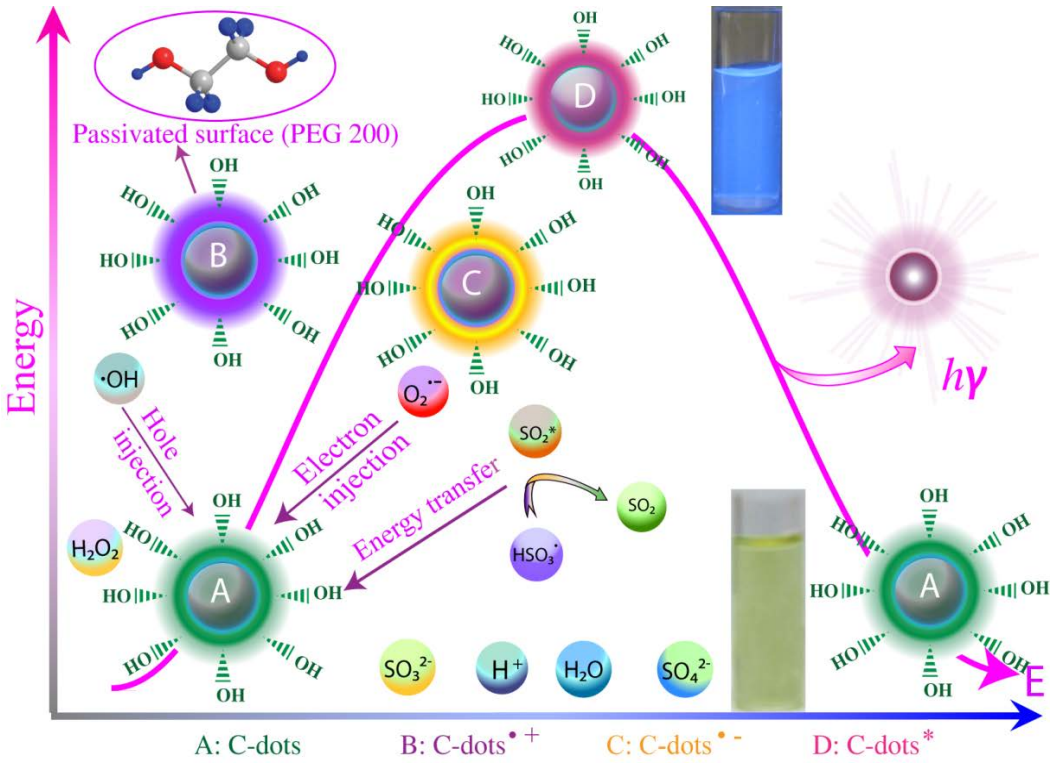

Fig. 6. Schematic illustration for the possible CL reaction mechanisms.

3.5 Analytical performance

As a means of analysis, inhibited CL system was often applied for sensitive trace analysis in different fields. Being having strong sensitization effects, C-dots were chosen as sensitizers of PHSA CL system for the detection of water soluble aliphatic primary amines (C1, C2, C3, C4, and C5). FIA CL analysis mode designed as Fig. 2 was employed in the test. Under the optimized conditions, calibration curves of relative CL intensities versus concentrations of the amines were obtained. The linear range was from 1×10^{-9} to 1×10^{-5} M (Table 2). All the equations showed good correlations. They demonstrated linear responses over the tested concentrations. The relative CL intensities had been subtracted the blank from the maximum peak. They increased linearly with the concentrations of amines. The relative standard deviations (R. S. D.) for 5 parallel determinations of five amines C1, C2, C3, C4, and C5 were 5.9%, 2.6%, 6.0%, 7.6% and 4.7% respectively. The detection limits achieved basing on 100 μL of solution of calibrators were also given in Table 2. Compared with the official method [49-51], the proposed method exhibited excellent agreements in detection limits. Fig. 7 displayed a typical FIA CL profile for the determination of standard amine solution with a concentration of 8×10^{-5} M. Under this same concentration, the strong CL signals of PHSA-C-dots system were increasingly inhibited with the increments of the carbon chains of amines (Fig. 7). This increasing trend was well consistent with the variation of reductive properties of the amines. The CL inhibition probably resulted from the reductive consumption of the oxidant H_2O_2 by amines during the CL reactions. The above

experiments indicated that the C-dots sensitized PHSA CL system could be used for the determination of aliphatic primary amines in water samples.**Table 2**. Analytical performance of the proposed inhibited CL system for the determination of water soluble aliphatic primary amines.

Analyte [a]	Linear range (M)	Calibration curve	Correlation coefficient	Detection limit (M)	
				Proposed method [b]	Official method
C1	2×10^{-7} to 1×10^{-5}	ΔI=15.5C+24.2	R2=0.998	3.3×10^{-9}	1.6×10^{-7}
C2	1×10^{-7} to 1×10^{-5}	ΔI=6.2C+63.4	R2=0.989	1.1×10^{-9}	1.8×10^{-8}
C3	1×10^{-8} to 1×10^{-6}	ΔI=56.6C+104.6	R2=0.988	3.3×10^{-10}	1.2×10^{-8}
C4	1×10^{-9} to 1×10^{-6}	ΔI=9.9C+138.6	R2=0.997	2.6×10^{-10}	5.5×10^{-8}
C5	1×10^{-9} to 1×10^{-6}	ΔI=84.9C+148.4	R2=0.998	2.5×10^{-10}	2.3×10^{-8}

[a] C1: methylamine, C2: ethylamine, C3: n-propylamine, C4: n-butylamine, and C5: n-pentylamine.

[b] Conditions: amine, 8×10^{-5} M , $KHSO_5$, Na_2SO_3 and HCl were all 1×10^{-2} M and the C-dots solution was 4×10^{-5} M; Flow rate : 1 mL min-1; High voltage, -0.8 KV.

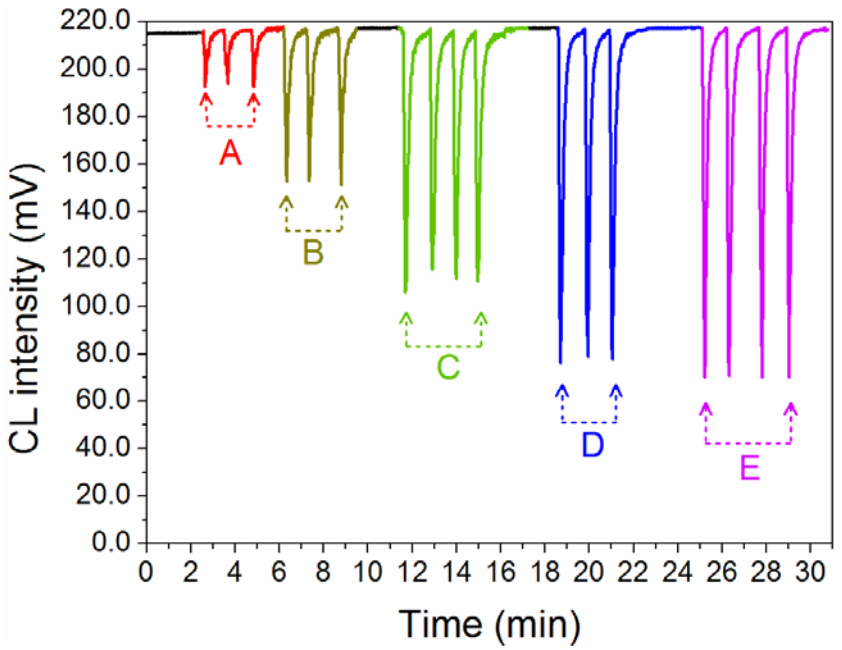

Fig. 7. A typical inhibited FIA CL profile for the determination of water soluble aliphatic primary amines (8×10^{-5} M). A: methylamine; B: ethylamine; C: n-propylamine; D: n-butylamine; and E: n-pentylamine. Analysis mode: Fig. 1B; Solutions of $KHSO_5$, Na_2SO_3 and HCl were all 1×10^{-2} M and the C-dots solution was 4×10^{-5} M; Flow rate : 1 mL min^{-1}; High voltage, -0.8 KV.

3.6 Inhibited CL determination of aliphatic primary amines

The proposed inhibited FIA CL system was then tested in real water samples with unknown amine concentrations. The water samples were labeled respectively as T1 (tap water), T2 (sewage), T3 (lotus pond water) and T4 (industrial wastewater from a factory). All the samples were collected, filtered through microporous membrane (aperture: 0.45 μm) and acidified to pH 2 with HCl. Prior to the analysis, the samples were alkalized to pH 10.5 with NaOH. The results were compared with the official values (Table 3) [135-137]. For sample T1 (tap water), no amines were detected. But for sample T4 (industrial wastewater from a factory), the results showed higher concentrations of amines than that of others, demonstrating severe amine contaminations in sample T4. Above results demonstrated that the C-dots sensitized PHSA CL system responded sensitively to water soluble aliphatic primary amines. It could be utilized as a rapid and sensitive detection system. After combined with other analysis techniques such as HPLC and CE, it could further be used for simultaneous detections of numerous compounds.

Table 3. Determination results for four water soluble aliphatic primary amines in real water samples.

Sample [a]	Method [b]	Found Concentration (ng ml^{-1})				
		C1	C2	C3	C4	C5
T1	Proposed	—	—	—	—	—
	Official	—	—	—	—	—
T2	Proposed	18.9	25.7	39.0	28.9	30.1
	Official	30	20.1	24	27	26.7
T3	Proposed	5.3	5.9	46.7	—	—
	Official	8.8	—	8.8	3.5	0.2
T4	Proposed	190.2	357.4	177.3	111.8	121.7
	Official	30	20	<5	<5	—

[a] T1: tap water, T2: sewage, T3: lotus pond water and, T4: industrial waste water from a factory.

[b] Conditions in proposed method: $KHSO_5$, Na_2SO_3 and HCl were all 1×10^{-2} M and the C-dots solution was 4×10^{-5} M; Flow rate: 1 mL min^{-1}; High voltage, -0.8 KV.

4 Conclusions

In summary, water soluble fluorescent C-dots were prepared. These C-dots had potential effects on PSHA CL system. TEM and ^{13}CNMR spectra indicated that C-dots had nanocrystalline cores inside and PEG 200 with hydrophilic groups of hydroxyl covered outside. UV spectra displayed a strong absorption spectra of C-dots at about 421 nm, while PL spectra of them showed a maximum emission at 502 nm. The CL enhancements of C-dots were supposed

to be originated from the processes of electron-transfer annihilation and resonance energy transfers. These transfers occurred between C-dots and active radicals produced by CL reactions of PSHA system. Aliphatic primary amines were able to inhibit CL signals of the C-dots sensitized PSHA CL system. Based on the findings, the C-dots sensitized PSHA CL system was then developed for the determination of aliphatic primary amines in real water samples. This work is important on the investigations of new and efficient catalysts for CL reactions. The C-dots sensitized CL system is promising in broadening analytical applications in various fields such as bioanalysis, catalysts, etc.

Chaterp 5 Conclusions

In the present work, three CL systems and its analytical application were investigated: 1 $KHSO_5$-$CoSO_4$ CL system, 2 L-cysteine capped Mn-doped ZnS quantum-dots enhanced NaClO-H_2O_2 CL system, and 3 C-dots sensitized PSHA CL system. The CL mechanism of ROS was also studied. The results indicated that:

1) Aliphatic dicarboxylic acids, such as oxalic acid, malonic acid, succinic acid, glutaric acid, hexane diacid and pimelic acid were found to enhance the $KHSO_5$-$CoSO_4$ CL signals. The CL enhancement of dicarboxylic acid might be attributed to the formation of peroxo-diacid, an unstable excited state, which finally decomposed to dicarboxylic acid and singlet oxygen. Moreover, the CL intensity was determined by the decomposition rate, which was improved with the increase of the carbon chain length. The CL signals were enhanced regularly with the increase of the carbon chain length. The CL emission was finally detected when the dimer $(^1O_2)_2^*$ being formed from singlet oxygen decayed to the triplet oxygen, a ground state species. Some organic compounds such as methanol were found to suppress the CL emission dramatically due to the scavenging of hydroxyl radical to $KHSO_5$-$CoSO_4$ system by methanol. This work was important for the CL mechanism investigation of $KHSO_5$-$CoSO_4$-dicarboxylic acid system.

2) The weak CL system of NaClO-H_2O_2 could be sensitized when it was induced by the sensitizer of Zn-dots. This sensitizer acted as an efficient catalysis center and an energy acceptor in CL resonance energy transfer process.

In the presence of sensitizer, the decomposition of H_2O_2 and the formation of monomol singlet oxygen ($^1O_2$) and excited dimol $(^1O_2)_2^*$ were promoted in the NaClO-H_2O_2 CL reactions; an energy transfer process occurred between donor of excited dimol singlet oxygen $(^1O_2)_2^*$ and acceptor of sensitizer. The CL signals of the NaClO-H_2O_2 system were finally enhanced dramatically by the sensitizer in the whole. This work was important for investigation of new and efficient catalysts of CL system and helpful for comprehension of CL mechanism correspondingly.

3) Water soluble fluorescent C-dots were prepared. These C-dots had potential effects on PSHA CL system. TEM and ^{13}CNMR spectra indicated that C-dots had nanocrystalline cores inside and PEG 200 with hydrophilic groups of hydroxyl covered outside. UV spectra displayed a strong absorption spectra of C-dots at about 421 nm, while PL spectra of them showed a maximum emission at 502 nm. The CL enhancements of C-dots were supposed to be originated from the processes of electron-transfer annihilation and resonance energy transfers. These transfers occurred between C-dots and active radicals produced by CL reactions of PSHA system. Aliphatic primary amines were able to inhibit CL signals of the C-dots sensitized PSHA CL system. Based on the findings, the C-dots sensitized PSHA CL system was then developed for the determination of aliphatic primary amines in real water samples. This work is important on the investigations of new and efficient catalysts for CL reactions. The C-dots sensitized CL system is promising in broadening analytical applications in various fields such as bioanalysis, catalysts, etc.

Chapter 6 Novelty statement

This work reported for the first time the preparations of Zn-dots and C-dots. The sensitizing effects of Zn-dots and C-dots on NaClO-H_2O_2 and PSHA CL systems respectively were also investigated for the first time. Finally, C-dots sensitized PSHA CL system were applied for the first time in analytical practice.

References

1. Alivisatos, A. P. Science 1996, 271, 933–937.
2. Chen, C. C.; Herhold, A. B.; Johnson, C. S.; Alivisatos, A. P. Science 1997,276, 398–401.
3. Peng, X. G.; Manna, L.; Yang, W.; Wickham, J.; Scher, E.; Kadavanich, A.;Alivisatos, A. P. Nature 2000, 404, 59–61.
4. He, Y.; Wang, H.-F.; Yan, X.-P. Anal. Chem. 2008, 80, 3832–3837.
5. Chen, X.; Dong, Y.; Fan, L.; Yang, D. Anal. Chim. Acta 2007, 582, 281–287.
6. Alivisatos, A. P. Science 1996, 271, 933–937.
7. Sun, Y.-P.; Zhou, B.; Lin, Y.; Wang, W.; Fernando, K. A. S.;Pathak, P.; Meziani, M. J.; Harruff, B. A.; Wang, X.; Wang, H. F.; Luo,P. G.; Yang, H.; Kose, M. E.; Chen, B. L.; Veca, L. M.; Xie, S.-Y. J. Am. Chem. Soc. 2006, 128, 7756–7757.
8. Xie, J. P.; Zheng, Y. G.; Ying, J. Y. J. Am. Chem. Soc. 2009,131, 888–889.
9. Yang, S.-T.; Cao, L.; Luo, P. G.; Lu, F. S.; Wang, X.; Wang, H. F.;Meziani, M. J.; Li, Y. F.; Qi, G.; Sun, Y.-P. J. Am. Chem. Soc. 2009,131, 11308–11309.
10. Li, H. T.; He, X. D.; Kang, Z. H.; Huang, H.; Liu, Y.; Liu, J. L.;Lian, S. Y.; Tsang, C. H. A.; Yang, X. B.; Lee, S. T. Angew. Chem., Int. Ed.2010, 49, 4430–4434.
11. Cao, L.; Sahu, S.; Anilkumar, P.; Bunker, C. E.; Xu, J.; Fernando,K. A. S.; Wang, P.; Guliant, E. A.; Tackett, K. N.; Sun, Y.-P. J. Am. Chem.Soc.

2011, 133, 4754–4757.

12. Navas, M. J.; Jim_enez, A. M. J. Agric. Food Chem. 1999, 47,183–189.

13. Lin, J.-M., Ed. Chemiluminescence: Principle and Applications;Chemical Industry Press: Beijing, 2004.

14. Chen, H.; Li, R. B.; Lin, L.; Lin, J.-M. Talanta 2010, 81,1688–1696.

15. J.H. Jang, H.B. Lim, Microchem. J. 94 (2010) 148.

16. W.R. Algar, M. Massey, U.J. Krull, Trends Anal. Chem. 28(2009) 292.

17. R. Narayanan, M.A. El-Sayed, J. Phys. Chem. B 109 (2005)12663.

18. Wang, H.-F.; He, Y.; Yan, X.-P. Anal. Chem. 2009, 81, 1615–1621.

19. Zheng, L.-Y.; Chi, Y. - W.; Dong, Y.-Q. J. Am. Chem. Soc. 2009,131, 4564–4565.

20. Yusuf G, Adewuyi, Samuel OO. *Ind. Eng. Chem. Res*. 2003; **42**(17): 4084–4100.

21. Ball DL, Edwards JOI. *J. Am. Chem. Soc.* 1956; **78**(6): 1125–1129.

22. Wang M, Zhao LX, Lin J-M. *Luminescence* 2007; **22**(2) : 182-188.

23. Richard JK, Albert MS. *J. Org. Chem*. 1960; **25**(11): 1901–1906.

24. Betterton EA, Hoffmann MR. *Environ. Sci. Technol*. 1990; **24**(12): 1819–1824.

25. Radziszewski, B. *Chem. Ber. 10*, **1877**, *70*, 321-332.

26. Dodeigne C, Thunus L, Lejeune R. *Talanta* 2000; **51**(3): 415-439.

27. Easton PM, Simmonds AC, Rakishev A, Egorov AM, Candeias LP. *J. Am. Chem. Soc*. 1996; **118**(28): 6619–6624.

28. Ruengsitagoon W, Liawruangrath S, Townshend A Talanta 2006; **69**(4):

976–983.

29. Yeh HC, Lin WY. *Talanta* 2003; **59**(5): 1029–1038.

30. Lu JZ, Lau CW, Lee MK, Kai M. *Anal. Chim. Acta* 2002; **455**(2): 193–198.

31. Liu YM, Cheng JK. *J. Chromatogr. A.* 2002; **959**(1): 1–13.

32. Powe AM, Fletcher KA, Luce NNS, Lowry M, Neal S, McCarroll ME, Oldham P. B, McGown LB. Warner, I. M. *Anal. Chem.* 2004; **76**(16): 4614–4634.

33. Roda A, Guardigli M, Michelini E, Mirasoli M, Pasini P. *Anal. Chem.* 2003 ; **75**(11) : 462A-470A.

34. Lin J-M, Yamada M. *Trends Anal. Chem.* 2003; **22**(2) : 99-107.

35. Zhang Z, Zhang S, Zhang X. *Anal. Chim. Acta* 2005; **541**(1): 37-47.

36. Liu ML, Zhao LX, Lin J-M*Phys. Chem. A.* 2006; **110**(23): 7509–7514.

37. Lu C, Lin J-M. *Catal. Today* 2004; **90**(4): 343–347.

38. Waseem A, Yaqoob M, Nabi A. *Luminescence* 2008; **23**(3) : 144-149.

39. Roebke W, Renz M, Henglein A. *Int. J. Radiat. Phys. Chem.* 1969; **1**(1): 39-44.

40. Zhu Q. *Luminescence* 2009; **24**(4) : 250-240.

41. Khan AU, Kasha M. Physical *J. Am. Chem. Soc.* 1966; **88**(7): 1574-1576.

42. Khan AU, Kasha M. *Nature* 1964; **204**(10): 241-243.

43. Khan AU, Kasha M. *J. Am. Chem. Soc.* 1970; **92**(11): 3293-3300.

44. Ness S, Hercules DM. *Anal. Chem.* 1969; **41**(11): 1467-1470.

45. Lu C, Song GQ, Lin J-M. *Trends Anal. Chem.* 2006; **25**(10): 985-995.

46. Anipsitakis GP, Stathatos E, Dionysiou DD. *J. Phys. Chem. B.* 2005; **109**(27): 13052-13055.

47. Muller JG, Zheng P, Rokita SE, Burrows CJ. *J. Am. Chem. Soc.* 1996; **118**(10): 2320-2325.

48. Asmus KD, MÖckel H, Henglein A*J. Phys. Chem.* 1973; **77**(10): 1218-1221.

49. Bothe E, Schulte FD. *Photochem. Photobio*. 1978; **28**(3): 639-644.

50. Silbert LS, Siegel E, Swern D. Peroxides. IX. *J. Org. Chem.* 1962, **27**(4): 1336-1342.

51. Koubek E, Haggett ML, Battaglia CJ, Ibne M, Pyun HY, Edwards JO. *J. Am. Chem. Soc.* 1963; **85**(15): 2263-2268.

52. Maruthamuthu P, Neta P. *J. Phys. Chem.* 1977; **81**(10): .937–940.

53. Zhang Z, Edwards JO. *Inorg. Chem.* 1992; **31**(17): 3514-3517.

54. Ouannes C, Wilson T. *J. Am. Chem. Soc.* 1968; **90**(23): 6527-6528.

55. Stephens ER, Hanst PL, Doerr RC. *Anal. Chem.* 1957; **29**(5): 776-777.

56. X. Michalet, F.F. Pinaud, L.A. Bentolila, J.M. Tsay, S. Doose, J.J. Li, G. Sundaresan, A.M. Wu, S.S. Gambhir, S. Weiss, Science 307 (2005) 538.

57. G. Harald, L. Markus, Science 329 (2010) 910.

58. L.C. Jorge, M. Manfred, M. Kathrin, H.D. Jan, M. Fabian, H.G. Lutz, A.J. Thomas, S. Meike, Science 325 (2009) 300.

59. J. Claudon, J. Bleuse, N.S. Malik, M. Bazin, P. Jaffrennou, N. Gregersen, C. Sauvan, P. Lalanne, J.M. Gérard, Nature 4 (2010) 174.

60. A.C. William, Nature 5 (2010) 710.

61. M. Bruchez, M. Moronne, P. Gin, S. Weiss, A.P. Alivisatos, Science 281 (1998) 2013.

62. Z. Eli, H.M.L. Piet, K. Ali, E.G. Hernán, I.H.B. Philippe, Nature, 7 (2010) 295.

63. A.P. Alivisatos, Science 271 (1996) 933.

64. D.Y. Wang, A.L. Rogach, F. Caruso, Nano Lett. 2 (2002) 857.

65. H. Mattoussi, J.M. Mauro, E.R. Goldman, G.P. Anderson, V.C. Sundar, F.V. Mikulec, M.G. Bawendi, J. Am. Chem. Soc. 122 (2000) 12142.

66. M. Raquel, G.G. Gustavo, T. Gloria, J. Phys. Chem. B 114 (2010) 10541.

67. S. Li, X. Zhang, W. Du, Y. Ni, X. Wei, J. Phys. Chem. C 113 (2009) 1046.

68. S. Li, X. Zhang, Z. Yao, R. Yu, F. Huang, X. Wei, J. Phys. Chem. C 113 (2009) 15586.

69. H. Chen, R. Li, L Lin, G. Guo, J.-M. Lin, Talanta 81 (2010) 1688.

70. C. Duan, H. Cui, Z. Zhang, B. Liu, J. Guo, W. Wang, J. Phys. Chem. C 111(2007) 4561.

71. Z. Zhang, H. Cui, M. Shi, Phys. Chem. Chem. Phys. 8 (2006) 1017.

72. T.K. Sau, A. Pal, T. Pal, J. Phys. Chem. B 105 (2001) 9266.

73. Z. Wang, J. Li, B. Liu, J. Hu, X. Yao, J. Li, J. Phys. Chem. B 109 (2005) 23304.

74. Y. Li, P. Yang, P. Wang, X. Huang, L. Wang, Nanotechnology 18 (2007) 225602.

75. J. Guo, H. Cui, J. Phys. Chem. C 111 (2007) 12254.

76. J. Guo, H. Cui, W. Zhou, W. Wang, J. Photochem. Photobiol. A 193 (2008) 89.

77. J.-M. Lin, M. Liu, J. Phys. Chem. B 112 (2008) 7850.

78. X. Huang, L. Li, H. Qian, C. Dong, J. Ren, Angew. Chem. Int. Ed. 118 (2006) 5264.

79. Z. Li, Y. Wang, G. Zhang, W.B. Xu, Y. Han, J. Lumin. 130 (2010) 995.

80. A. Wolcott, D. Gerion, M. Visconte, J. Sun, A. Schwartzberg, S. Chen, J.Z. Zhang, J. Phys. Chem. B 110 (2006) 5779.

81. A.R. Clapp, I.L. Medintz, H. Mattoussi, ChemPhysChem. 7 (2006) 47.

82. J.K. Jaiswal, S.M. Simon, Trends Cell Biol. 14 (2004) 497.

83. H. F. Wang, Y. He, T. R. Ji, X. P. Yan, Anal. Chem. 81(2009) 1614.

84. J.-M. Lin, M. Yamada, Anal. Chem. 72 (2000) 1148.

85. L. Eberson, Electron Transfer Reactions in Organic Chemistry, vol. 25. Springer Verlag: Berlin. 1987.

86. R. Castagna, J.P. Eiserich, M. S. Budamagunta, P. Stipa, C.E. Cross, E. Proietti, J.C. Voss, L. Greci, Atmos. Environ. 42 (2008) 6551.

87. Y. P. Sun, B. Zhou, Y. Lin, W. Wang, K. A. S. Fernando, P. Pathak, M. J. Meziani, B. A. Harruff, X. Wang, H. F. Wang, P. G. Luo, H. Yang, M. E. Kose, Chen, L. B. M. L. Veca, S. Y. Xie, J. Am. Chem. Soc. 128 (2006) 7756-7757.

88. S. T. Yang, L. Cao, P. G. Luo, F. S. Lu, X. Wang, H. F. Wang, M. J. Meziani, Y. F. Liu, G. Qi, Y. P. Sun, J. Am. Chem. Soc. 131 (2009) 11308-11309.

89. L. Cao, X. Wang, M. J. Meziani, F. S. Lu, H. F. Wang, P. G. Luo, Y. Lin, B. A. Harruff, L. M. Veca, D. Murray, S. Y. Xie, Y. P. Sun, J. Am. Chem. Soc. 129 (2007) 11318-11319.

90. S. T. Yang, X. Wang, H. F. Wang, F. S. Lu, P. G. Luo, L. Cao, M. J. Meziani, J. H. Liu, Y. F. Liu, M. Chen, Y. P. Huang, Y. P. Sun, J. Phys. Chem. C 113 (2009) 18110-18114.

91. L. Tian, D. Ghosh, W. Chen, S. Pradhan, X. J. Chang, S. Chen, Chem. Mater. 21 (2009) 2803-2809.

92. Q. L. Zhao, Z. L. Zhang, B. H. Huang, J. Peng, M. Zhang, D. W. Pang, Chem. Commun. (2008) 5116-5118.

93. X. Y. Xu, R. Ray, Y. L. Gu, H. J. Ploehn, L. Gearheart, K. Raker, W. A. Scrivens, J. Am. Chem. Soc. 126 (2004) 12736-12737.

94. L. Y. Zheng, Y. W. Chi, Y. Q. Dong, J. P. Lin, B. B. Wang, J. Am. Chem. Soc. 131 (2009) 4564-4565.

95. X. H. Wang, K. G. Qu, B. L. Xu, J. S. Ren, X. G. Qu, X. H. Wang, J. Mater. Chem. 21 (2011) 2445-2450.

96. H. Zhu, X. L. Wang, Y. L. Li, Z. J. Wang, F. Yang, X. R. Yang, Chem. Commun. (2009) 5118-5120.

97. F. Wang, S. P. Pang, L. Wang, Q. Li, M. Kreiter, C. Y. Liu, Chem. Mater. 22 (2010) 5895-5899.

98. V. Wood, J. E. Halpert, M. J. Panzer, M. G. Bawendi, V. Bulovic, Nano Lett. 9 (2009) 2367-2375.

99. R. L. Liu, D. Q. Wu, S. H. Liu, K. Koynov, W. Knoll, Q. Li, Angew.

Chem. Int. Ed. 48 (2009) 4598-4601.

100. S. L. Hu, K. Y. Niu, J. Sun, J. Yang, N. Q. Zhao, X. W. Du, J. Mater. Chem. 19 (2009) 484-488.

101. J. G. Zhou, C. Booker, R. Y. Li, X. T. Zhou, T. K. Sham, X. L. Sun, Z. F. Ding, J. Am. Chem. Soc. 129 (2007) 744-745.

102. H. Peng, J. T. Sejdic, Chem. Mater. 21 (2009) 5563-5565.

103. H. P. Liu, T. Ye, C. D. Mao, Angew. Chem. Int. Ed. 119 (2007) 6593-6595.

104. A. B. Bourlinos, A. Stassinopoulos, D. Anglos, R. Zboril, V. Georgakilas, E. P. Giannelis, Chem. Mater. 20 (2008) 4539-4541.

105. X. Wang, L. Cao, S. T. Yang, F. S. Lu, M. J. Meziani, L. L. Tian, K. W. Sun, M. A. Bloodgood, Y. Pi. Sun, Angew. Chem. Int. Ed. 49 (2010) 5310-5314.

106. F. Wang, Y. H. Chen, C. Y. Liu, D. G. Ma, Chem. Commun. 47 (2011) 3502-3504.

107. Q. Li, T. Y. Ohulchanskyy, R. L. Liu, K. Koynov, D. Q. Wu, A. Best, R. Kumar, A. Bonoiu, P. N. Prasad, J. Phys. Chem. C 14 (2010) 12062-12068.

108. S. C. Ray, A. Saha, N. R. Jana, R. Sarkar, J. Phys. Chem. C 113 (2009) 18546-18551.

109. Y. P. Sun, X. Wang, F. S. Lu, L. Cao, M. J. Meziani, P. G. Luo, L. R. Gu, L. M. V. Chen, J. Phys. Chem. C 112 (2008) 18295-18298.

110. S. H. Lee, G. Jo, W. Park, S. Lee, Y. S. Kim, B. K. Cho, T. Lee, W. B. Kim, J. Phys. Chem. C 113 (2009) 18546-18551.

111. L. W. Li, D. Bedrov, G. D. Smith, J. Phys. Chem. B 110 (2006) 10509-10513.

112. H. T. Li, X. D. He, Z. H. Kang, H. Huang, Y. Liu, J. L. Liu, S. Y. Lian, C. H. A. Tsang, X. B. Yang, S. T. Lee, Angew. Chem. Int. Ed. 122 (2010) 4532-4536.

113. P. Simon, C. Lemacon, Anal. Chem. 59 (1987) 480-484.

114. M. T. Chiang, M. C. Lu, C. W. Whang, Electrophoresis 24 (2003) 3033-3039.

115. R. Freeman, X. Q. Liu, I. Willner, J. Am. Chem. Soc. 133 (2011) 11597-11604.

116. M. Matsumoto, H. Suzuki, N. Watanabe, H. K. Ijuin, J. Tanaka, C. Tanaka, J. Org. Chem. C 76 (2011) 5006-5017.

117. S. Bi, J. L. Zhang, S. Y. Hao, C. F. Ding, S. S. Zhang, Anal. Chem. 83 (2011) 3696-3702.

118. L. Roda, M. Mirasoli, L. S. Dolci, A. Buragina, F. Bonvicini, P. Simoni, M. Guardigli, Anal. Chem. 83 (2011) 3178-3185.

119. O. Jilani, T. M. Donahue, M. O. Mitchell, J. Chem. Educ. 88 (2011) 786-787.

120. S. C. Donhauser, R. Niessner, M. Seidel, Anal. Chem. 83 (2011) 3153-3160.

121. Y. M. Liu, L. Mei, L. J. Liu, L. F. Peng, Y. H. Chen, S. W. Ren, Anal. Chem. 83 (2011) 1137-1143.

122. L. Q. Fang, H. Chen, X. T. Ying, J.-M. Lin, Talanta 84 (2011) 216-222.

123. X. L. Chen, C. Wang, X. M. Tan, J. Wang, Anal. Chim. Acta 689 (2011) 92-96.

124. D. L. Ball, J. Edwards, J. Am. Chem. Soc. 78 (1956) 1125-1129.

125. S. Han, C. Y. Kim, D. Kwon, Polym. Degrad. Stab. 47 (1995) 203-208.

126. G. Yusuf, S. O. Adewuyi, Ind. Eng. Chem. Res. 42 (2003) 4084-4100.

127. G. V. Buxton, A. Elliot, L. A. Wall, J. Am. Chem. Soc., Faraday Trans. 89 (1993) 485-488.

128. V. M. James, R. H. Michael, J. Phys. Chem. 87 (1983) 5245-5249.

129. K. V. Vladimir, J. Phys. Chem. A 102 (1998) 601-605.

130. C. Sun, B. Liu, J. Li, Talanta 75 (2008) 447-454.

131. J.-M. Lin, T. Hobo, Anal. Chim. Acta 323 (1996) 69-74.

132. C. J. Miller, A. L. Rose, T. D. Waite, Anal. Chem. 83 (2011) 261-268.

133. Z. F. Ding, B. M. Quinn, S. K. Haram, L. E. Pell, B. A. Korgel, A. J. Bard, Science. 296 (2002) 12933-1297.

134. Z. Lin, W. Xue, H. Chen, J.-M. Lin, Anal. Chem. 83 (2011) 8245-8251.

135. S. M. Lloret, C. M. Legua, J. V. Andrés, P. C. Falcó, J. Chromatogr. A 1035 (2004) 75-82.

136. F. Sachet, S. Lenz, H. J. Brauch, J. Chromatogr. A 764 (1997) 85-93.

137. Y. Hui, L. Zhou, X. G. Chen, Talanta 80 (2010) 1619-1625.

Acknowledgements

The author wish to express his sincerely gratitude to my supervisors, Prof. Nobuaki Ogawa and Prof. Jin-Ming Lin who were abundantly helpful and offered invaluable assistance, support and guidance. Special thanks also to all my graduate friends, especially group members; Hui Chen, Zhen Lin, Junxiao Liu, Wei Xue, Jingmin Qiu, and Gaowa Xing for sharing the literature and invaluable assistance. The author would also like to convey thanks to the National Natural Science Foundation of China (No. 20935002, 90813015 and 20775042) and 863 Program of China (No. 2007AA09210107) for providing the financial means and laboratory facilities. The author wishes to express his love and gratitude to his beloved families; for their understanding & endless love, through the duration of his studies.

List of Publication

1）Yun **Zhou**, Gaowa Xing, Hui Chen, Nobuaki Ogawa, Jin-Ming Lin, Carbon nanodots sensitized chemiluminescence on peroxomonosulfate-sulfite-hydrochloric acid system and its analytical applications, *Talanta*, **2012**, 99, 471-477.

2）Zhen Lin, Hui Chen, **Yun Zhou**, Nobuaki Ogawa, Jin-Ming Lin, Self-catalytic degradation of *ortho*-chlorophenol with fenton's reagent studied by chemiluminescence, *J. Environ. Sci.*, **2012**, 24(3), 551-558.

3）**Yun Zhou**, Nobuaki Ogawa, Jin-Ming Lin, Enhanced chemiluminescence of peroxomonosulphate-cobalt (II) system in the presence of dicarboxylic acids, *Luminescence*, **2011**, 26, 280-288.

4）**Yun Zhou,** Hui Chen, Nobuaki Ogawa, Jin-Ming Lin, Chemiluminescence from NaClO-H_2O_2 and enhanced by L-cysteine capped Mn-doped ZnS quantum-dots, *Journal of Luminescence*, **2011**, 131, 1991-1997.

5）Jingmin Qiu, **Yun Zhou**, Hui Chen, Jin-Ming Lin, Immunomagnetic separation and rapid detection of bacteria using bioluminescence and microfluidics, *Talanta*, **2009**, 79, 787-795.

6）**周云**，刘军晓，林金明，掺锰ZnS量子点对NaClO-H_2O_2体系的化学发光增强作用研究（口头报告），第十届中国化学会分析化学年会暨第十届全国原子光谱学术会议，扬州大学, 2009 年 10 月 30 日－11 月 1 日.

7）Jingmin Qiu, **Yun Zhou**, Hui Chen, Jin-Ming Lin, Immunomagnetic separation and rapid detection of bacteria using bioluminescence and microfluidics (Poster), 24th MSB2009, Dalian, China, October 19-22, 2009.

8）**Yun Zhou**, Jun-Xiao Liu, Jin-Ming Lin, Sensitized chemiluminescence of Mn-doped ZnS quantum-dots on NaClO-H_2O_2 system (Poster), The Second China-Canada Symposium on Analytical Chemistry for Life Sciences, Beijing, China, October 14-17, 2009.

9）**周云**，祁光霞，李兆陇. 跨学科、开放性分析实验：餐厨垃圾厌氧发酵沼液中蛋白质含量的测定. 第八届大学生化学实验邀请赛教学研讨会论文集, 2012 年，上海.

Brief Introduction of Author

The author Yun Zhou was born in a family of farmers at village in Hubei Province, China, on February 6th, 1974. He graduated from Hubei University in 1998 and got bachelor's degree in chemical education. In the ensuing three years, he taught in a high school of Wuhan city, Hubei province. He got master's degree in chemistry from the Huzhong University of Science and Technology in 2004. Even after working in Chemistry Department of Tsinghua University, he continued his education and carried out chemical research work in the group of Dr. Prof. Jin-Ming Lin.

He was very keen on his work and achieved 20 awards from schools and municipal education ministry. He was very interested in chemical research, especially in CL research. So far, he has 5 original SCI papers and 9 symposium presentations. In addition, he participated in writing of two books on chemistry and biochemistry.